ΕΛΛΗΝΙΚΟ ΜΕΣΟΓΕΙΑΚΟ ΠΑΝΕΠΙΣΤΗΜΙΟ
Σχολή Ηλεκτρολόγων Μηχανικών

Διατμηματικό πρόγραμμα μεταπτυχιακών σπουδών

Προηγμένα Συστήματα Παραγωγής, Αυτοματισμού & Ρομποτικής

ΜΕΤΑΠΤΥΧΙΑΚΗ ΔΙΠΛΩΜΑΤΙΚΗ ΕΡΓΑΣΙΑ

Ευφυής ρομποτική κάμερα ενός άξονα για τη συλλογή εικόνων και την παρακολούθηση της ανάπτυξης φυτών σε μελέτες γεωργίας ακριβείας.

Περδικάκης Σπυρίδων ΜΤΗ114

Επιβλέπων: Δρ. Παναγιωτάκης Σπυρίδων

Ηράκλειο Κρήτης
Απρίλιος 2023

HELLENIC MEDITERRANEAN UNIVERSITY
School of Electrical Engineering

Postgraduate Program

Master of Science in Advanced Manufacturing Systems, Automation and Robotics

MASTER THESIS

Smart robotic single axis camera for the collection of images and the monitoring of plant growth in studies of precision agriculture.

Perdikakis Spyridon

Advisor: Dr. Panagiotakis Spyridon

Heraklion, Crete
April 2023

Αν θες να είσαι καλός άνθρωπος,
μην κάνεις στους άλλους ό,τι δε θα ήθελες να σου κάνουν.
Αν θες να αγιάσεις,
κάνε στους άλλους ό,τι θα ήθελες να σου κάνουν…

Abstract

Monitoring plants and acquiring data in a greenhouse is a task that requires significant effort and time.

Achieving the necessary accuracy and repeatability in plant image acquisition can be challenging.
To address this issue, it is essential to implement a robotic system that can acquire images of the plants at any time of the day or night, at the precise spot and angle, without the need for human presence, which would improve efficiency and reduce labor costs. The images captured can be transmitted to a remote computer, enabling researchers to effortlessly monitor plant health.

The goal of this thesis project, is the construction and programming of a one axis robotic arrangement that can systematically detect and take images of plants, both in the visible and infrared spectrum, for the purpose of their automated monitoring of development, enabling remote decision-making for their health and their protection from diseases.

This way, the researcher can monitor the growth and health of the plants in the greenhouse without physically being present.

Περίληψη

Η παρακολούθηση φυτών και η απόκτηση δεδομένων σε ένα θερμοκήπιο είναι μια εργασία που απαιτεί σημαντική προσπάθεια και χρόνο.

Η επίτευξη της απαιτούμενης ακρίβειας και επαναληψιμότητας στη λήψη εικόνων φυτών μπορεί να αποτελέσει πρόκληση. Για να αντιμετωπιστεί αυτό το ζήτημα, είναι απαραίτητο να υλοποιηθεί ένα ρομποτικό σύστημα που μπορεί να λάβει εικόνες των φυτών οποιαδήποτε ώρα της ημέρας ή της νύχτας, στο σωστό σημείο και γωνία, χωρίς την ανάγκη ανθρώπινης παρουσίας, βελτιώνοντας την απόδοση και μειώνοντας το κόστος εργασίας. Οι εικόνες αυτές μπορούν να μεταδοθούν σε ένα απομακρυσμένο υπολογιστή, δίνοντάς μας τη δυνατότητα να παρακολουθήσουμε τα φυτά.

Ο στόχος αυτής της εργασίας είναι η κατασκευή και η προγραμματισμός ενός ρομποτικού συστήματος ενός άξονα, που μπορεί συστηματικά να ανιχνεύει και να λαμβάνει εικόνες φυτών, τόσο στο ορατό όσο και στο υπέρυθρο φάσμα, για τον σκοπό της αυτόματης παρακολούθησης της ανάπτυξής τους, επιτρέποντας τη λήψη αποφάσεων από απόσταση, για την υγεία και την προστασία τους από ασθένειες. Με αυτόν τον τρόπο, ο ερευνητής μπορεί να παρακολουθεί την ανάπτυξη και την υγεία των φυτών στο θερμοκήπιο χωρίς να είναι απαραίτητη η φυσική του παρουσία.

Acknowledgments

I have to start by thanking my family. In order to complete my master's degree, I had to be absent for hundreds of hours. My wonderful children never complained, and my awesome wife lifted the weight of handling all the family matters that I couldn't. All of them have been extremely supportive, telling me how proud I made them.

My colleagues, together we managed to successfully complete the courses, after a lot of team effort and cooperation.

My teachers, they all have been excellent at their work, and I gained extremely useful knowledge from them.

Dr. Daliakopoulos Ioannis, who gave me the idea of this thesis, directives about how the device should operate and secured the funding for the parts required for the robotic camera. Part of this work was co-financed by the European Union and Greek national funds through the Operational Program Competitiveness, Entrepreneurship and Innovation, under the call RESEARCH - CREATE - INNOVATE (project SOilless culture UPgrade – SOUP code:T1EDK-04171).

Papadimitriou Dimitrios. He has been very helpful, providing me with the necessary pots, plants etc. He has always been available when I needed to visit the greenhouse, and took care of the plants for me, transferring them from the greenhouse to the lab and back, many times.

My supervisor, Dr. Panagiotakis Spyridon, who apart from being a great teacher, he consulted me into taking the work I've made for this thesis a step further, bringing me together with Dr. Zacharias Kamarianakis.

Dr. Kamarianakis Zacharias, with his help, I gained the experience of making a research paper publication. We have been working closely together for over a year, and apart from learning from him new for me scientific methods, I made a very good friend.

Table of Contents

List of Tables

List of Equations

List of Figures

List of Images

1. Introduction

1.1. Motivation

Agriculture was first invented about 12,000 years ago, which was a period of time when humans began to transition from a hunter-gatherer lifestyle to a settled, agricultural lifestyle (Wikipedia: History of agriculture , n.d.).

In Rome in 30 A.D. when Emperor Tiberius became sick and was prescribed to eat one cucumber a day, a room with stone walls for insulation and glass ceilings to let in light was built. Cucumbers were planted in wheeled carts which were put in the sun daily, then taken inside to keep them warm at night (Wikipedia: Greenhouse, n.d.). The greenhouse had just been invented.

Since then, greenhouses have been used to provide a controlled environment for plant growth, regardless of the weather or season. Greenhouses allow growers to manipulate temperature, humidity, light, and other environmental factors to optimize plant growth and yield. By providing protection from harsh weather conditions, pests, and diseases, greenhouses create a favorable environment for crops to thrive. They also enable growers to extend the growing season and cultivate plants that may not be able to survive in the local climate otherwise.

In the recent years, by the advancement of technology, precision agriculture has risen and has been increasingly used in greenhouses.

A robotic system with cameras and sensors can bring significant benefits to precision agriculture in greenhouses. By combining the capabilities of cameras and sensors, this system can provide growers with accurate data on plant growth and health, allowing them to optimize growing conditions and improve crop quality and consistency.

Such a system can automate capturing of high-resolution images of individual plants. These images can then be analyzed to identify trends and make data-driven decisions about fertilization and pruning, improving crop yield and quality. This level of automation reduces the need for manual labor and can lead to lower labor costs and a more efficient operation, achieving the necessary accuracy and repeatability in plant image acquisition from the exact same spot and angle, any time of the day or night, without the need for human presence.

Furthermore, a robotic camera can send the images captured to a remote computer, enabling growers to remotely identify plant stress and disease at an early stage, thus taking action to prevent crop loss.

Such a robotic camera has been implemented in this master thesis project, that was undertaken on behalf of the researchers at the Faculty of Agriculture of the Hellenic Mediterranean University, who required a robotic camera system that could autonomously locate and monitor lettuce plants in pots. The project involved designing and implementing a robotic camera that could carry out this task in the greenhouse of the Hellenic Mediterranean University [Image 1]. The researchers provided the necessary equipment and resources for the successful completion of the project.

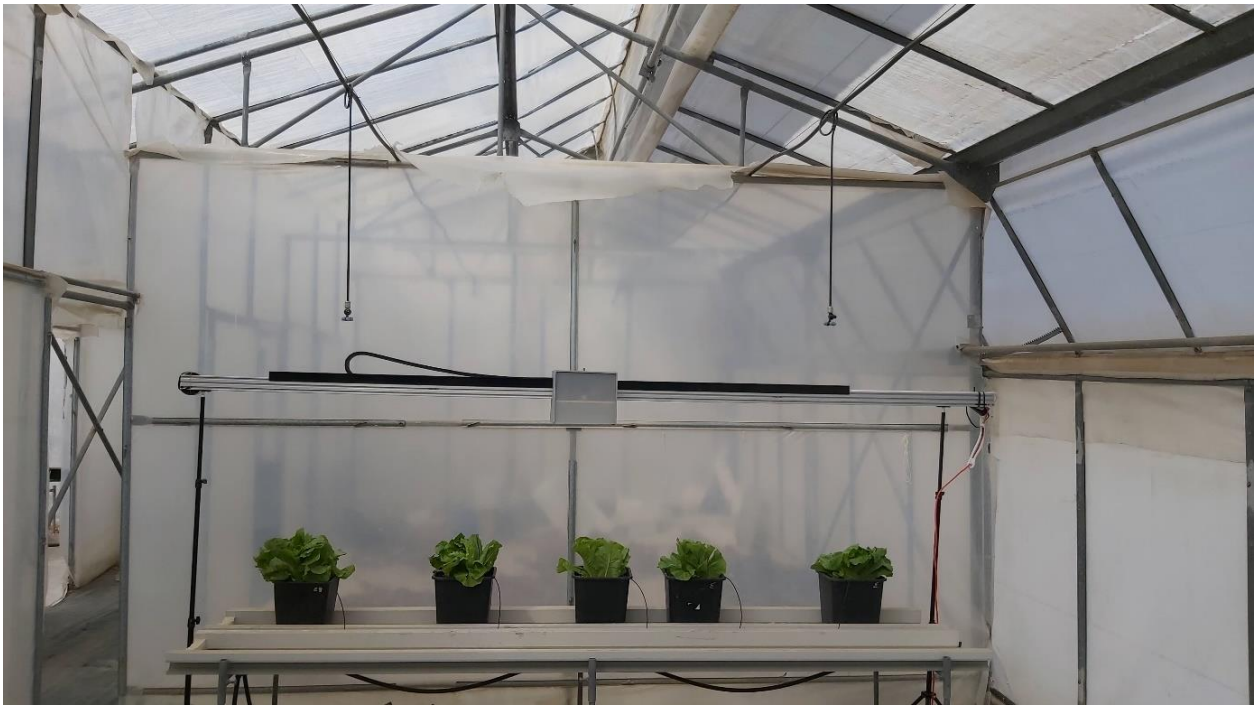

Image 1.
The Greenhouse

1.2. Thesis structure

The thesis comprises a total of eight chapters, each serving a specific purpose in advancing the thesis's overarching goal.

Chapter 1 sets the stage for the thesis by providing a concise introduction that contextualizes the problem under investigation.

Chapter 2 provides an overview of related technologies and work of precision agriculture in greenhouses, covered in magazines and websites, as well as research papers. Moreover, the chapter delves into HSV color space, the visible spectrum, infrared spectrum, and NDVI for plant identification, as well as multi-exposure image fusion (MEF) to produce high dynamic range (HDR) images.

Chapter 3 discusses the design of the system, with a focus on requirement analysis, design considerations and the hardware and software that was selected and utilized. The chapter goes into great detail on the hardware components, such as the metal structure, moving parts, sensors, illumination LEDs, power supplies, switches, cameras, Raspberry Pi computational unit and electronic components. The software tools utilized are also discussed, with a focus on OpenCV, Syncthing continuous file synchronization, and remote desktop software.

Chapter 4 covers the implementation of the system, with a focus on the schematic and PCB, hardware assembly software development and plant's width calculation. The chapter goes into detail on how the system was set up, the carriage's movement, the user interface, lens distortion correction, the system's initialization and parameterization, homing, and how the timer for repeated plant recognition and acquisition is implemented.

Chapter 5 evaluates the performance of the robotic system in terms of its movement and plant identification precision. The chapter provides a comprehensive analysis of the experiments conducted to evaluate the system's capabilities and reports on the results that were obtained.

In **Chapter 6**, an experiment of plant growth monitoring is reported, and Multi-exposure image fusion (MEF) producing High Dynamic Range Imaging (HDR) images, as well as NDVI is discussed. Both MEF and NDVI have been tested, and the experiments conducted are reported here.

Chapter 7 synthesizes the thesis's findings and draws general conclusions. This chapter summarizes the key findings of the thesis, identifies any limitations or challenges encountered during the research, and presents potential solutions to these issues.

Finally, in **Chapter 8**, the thesis identifies areas for future research and development. As the system developed in this thesis has vast potential, this chapter serves as a springboard for identifying new avenues for scientific inquiry.

The thesis ends with a list of references.

2. Overview of related technologies and work

There are several state-of-the-art technologies being used in greenhouses today that are reported in the literature. In the next sections, some of them have been collected that are quite relevant to this work. Section 2.1 focuses on publications published in various informational web sites and online technological magazines and Section 2.2 focuses on research papers. Then, 2.3 pays attention to some related technologies that will be used in this study.

2.1. Magazines and web sites

An example is AppHarvest's greenhouse in Appalachia, Kentucky, which is the biggest in the US. Using artificial intelligence (AI) and robotics, the company says it yields 30 times more per acre than open fields while using 90% less water (CNN World: Is the biggest greenhouse in the US the future of farming?, n.d.).

The facility collects data from the plants using 300 sensors, and growers can remotely monitor the microclimate to ensure that crops receive the ideal amount of nutrients and water [Image 2].

Image 2.
Robotic sprayers
source: (CNN World: Is the biggest greenhouse in the US the future of farming?, n.d.)

Artificial intelligence analyzes data from over 700,000 plants, and data is also collected by cameras attached to Virgo, AppHarvest's AI-powered robot. Virgo uses AI to assess which tomatoes are ripe enough to harvest and then picks and prunes them with its robotic arm [Image 3].

Image 3.
Robotic system with cameras harvesting ripe tomatoes
source: (CNN World: Is the biggest greenhouse in the US the future of farming?, n.d.)

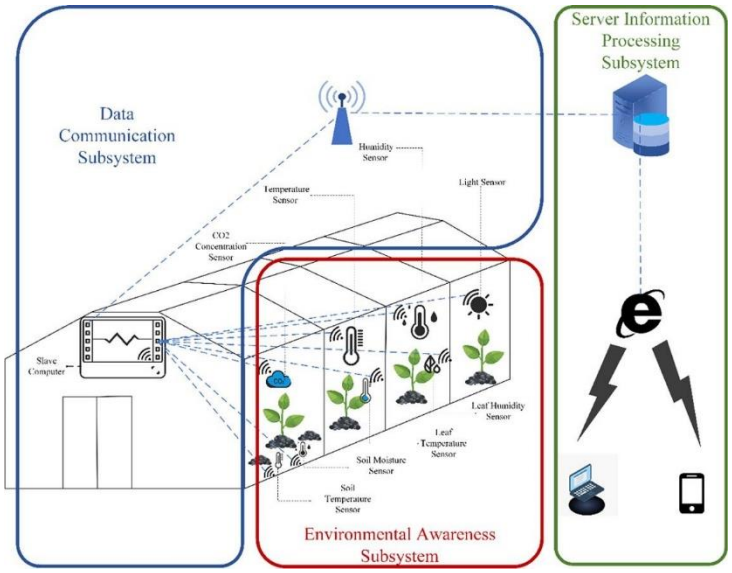

Figure 1.
Towards automated greenhouse: A state of the art review on greenhouse monitoring methods and technologies based on internet of things.
source: Li et al. (2021)

Some other examples of state-of-the-art technologies being used in greenhouses today include the use of internet of things (IoT) for environmental monitoring. A review of Li et al. (2021) on greenhouse monitoring methods and technologies based on IoT found that multi-parameter monitoring is beneficial to achieve effective greenhouse control, and wireless technology has gradually replaced wired mode for data transmission in the environment both inside and outside the greenhouse [Figure 1].

Notably, deep learning, big data, and other advanced technologies used in greenhouse monitoring are considered valuable developments, further refining unmanned greenhouse management and further improving greenhouse construction's energy utilization.

2.2. Research papers

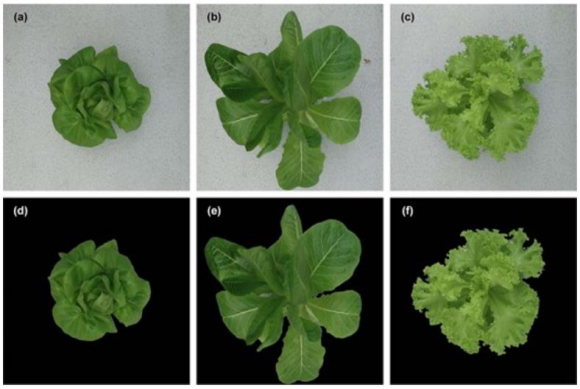

Image 5.
a–c shows the original images of greenhouse lettuce, and d–f shows the corresponding segmentation results
source: Zhang et al. (2020)

Image 4.
Processing of a leaf samples with ImageJ
source: Moschou et al. (2022)

Combining computer vision and robotics can offer a range of benefits for growers in monitoring the growth and health of plants in greenhouses. In recent years, several studies have explored the potential of computer vision and deep learning techniques in this context. One such study by Zhang et al. (2020) used a convolutional neural network (CNN) to monitor the growth of lettuce in a greenhouse [Image 5]. The CNN was trained to recognize and classify different stages of lettuce growth based on images taken by cameras in the greenhouse. The results showed that the CNN achieved high accuracy in monitoring the growth of lettuce.

Another study by Bauer et al. (2019) explored the use of computer vision and deep learning techniques for ultra-scale aerial phenotyping and precision agriculture. In this study, the researchers used a combination of aerial images, ground-based sensors, and

machine learning algorithms to monitor the growth of lettuce. The results showed that this approach could accurately predict plant traits such as leaf area and dry weight.

Kosmopoulos et al. (2020) discuss the current state and future activities of the SOUP project (SOilless culture UPgrade), which aims to automate the monitoring of plant growth through sensor networks, and to introduce robotic technology for the labor-intensive tasks such as pest management and harvesting. Specifically, the project investigates the cultivation of tomatoes.

Kounalakis et al. (2021) present their work on the development of a tomato harvesting robot that can recognize and approach tomato peduncles using computer vision techniques. The detection and approach procedure was found to be 65%, with 92.6% accuracy of the vision processing in locating the correct cutting point.

Georgantopoulos et al. (2023) introduce a dataset of multispectral images (RGB and NIR) of tomato plants, at various stages of infection with two common tomato pests, Tuta Absoluta and Leveillula Taurica, using machine learning algorithms.

Image 6.
Augmented output data (left to right): (a) original, (b) width shift, (c) height shift, (d) shear, (e) horizontal flip, (f) vertical flip, and (g) zoomed in
source: Ahsan et al. (2022)

To further improve the growth of plants in greenhouses, researchers made use of (manual, or semi-manual) measuring leaf size (and other plant dimensions) as an indicator of yield/plant growth. Researchers have also explored the use of alternative hydroponic growing media. For example, Moschou et al. (2022) used grocery waste compost as a hydroponic growing medium for lettuce [Image 4]. The study found that the use of compost as a growing medium improved the growth and quality of lettuce, while also reducing waste.

The Internet of Things (IoT) has revolutionized precision agriculture in greenhouses, allowing growers to monitor and control various environmental factors with greater accuracy and efficiency. With IoT sensors installed throughout the greenhouse, growers can collect data on temperature, humidity, soil moisture, light levels, and other important variables in real-time. This data can be analyzed and used to automate the greenhouse's systems, such as irrigation, lighting, and ventilation, to create optimal growing conditions for crops. IoT technology has also enabled remote monitoring and control, giving growers the ability to manage their greenhouse operations from anywhere, at any time.

This thesis' robotic camera called "RoboPlantDect", has been designed to be able to make use of IoT connected sensors in the future, like Nikoloudakis et al. (2018) have. They introduced a novel cloud service that works with specialized Internet of Things (IoT)-based composting machinery to allow for unsupervised composting. Nikoloudakis et al. (2016) researched about composting and its management using a virtualized cloud-based system. Also, Fragkopoulos et al. (2023) review the crucial factors that affect communication performance of the LoRaWAN protocol which is widely used in IoT greenhouse applications.

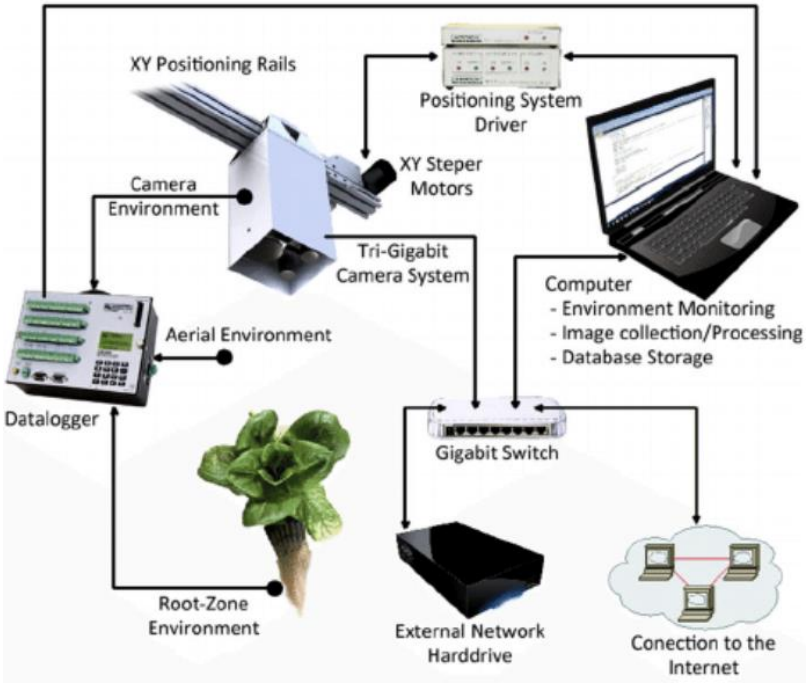

Figure 2.
Computer vision-guided crop diagnostics system components. source: David Story et al. (2015)

In addition to monitoring growth, computer vision and robotics can also help in detecting nutrient deficiencies in plants. Kamarianakis et al. (2023) designed and implemented a chlorophyll content meter, which utilizes low cost components. Another study by Ahsan

et al. (2022) used deep learning models to determine nutrient concentrations in hydroponically grown lettuce cultivars [Image 6]. The researchers used a combination of computer vision techniques and machine learning algorithms to accurately predict the nutrient concentrations of different lettuce cultivars.

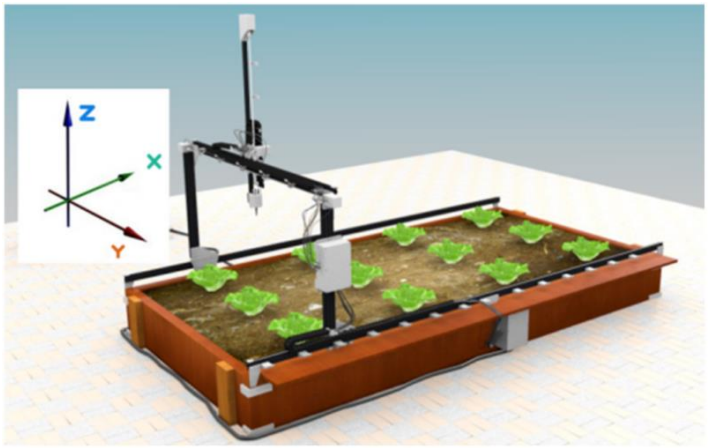

Figure 3.
Plain schematic of CityVeg's layout source: Moraitis et al. (2022)

Robotics can also play a key role in monitoring plant health in greenhouses. For example, Moraitis et al. (2022) designed and implemented an urban farming robot named "CityVeg" that could move autonomously around a fixed bed, a "garden parcel" as they call it, monitor plant health, and perform tasks such as watering and fertilizing [Figure 3]. The robot was equipped with a range of sensors and cameras to detect plant health and growth. David Story et al. (2015) designed and implemented a computer vision-guided greenhouse crop diagnostics system [Figure 2]. The system uses a camera to capture images of the plants and then applies image processing techniques to extract features from the images, such as color and texture.

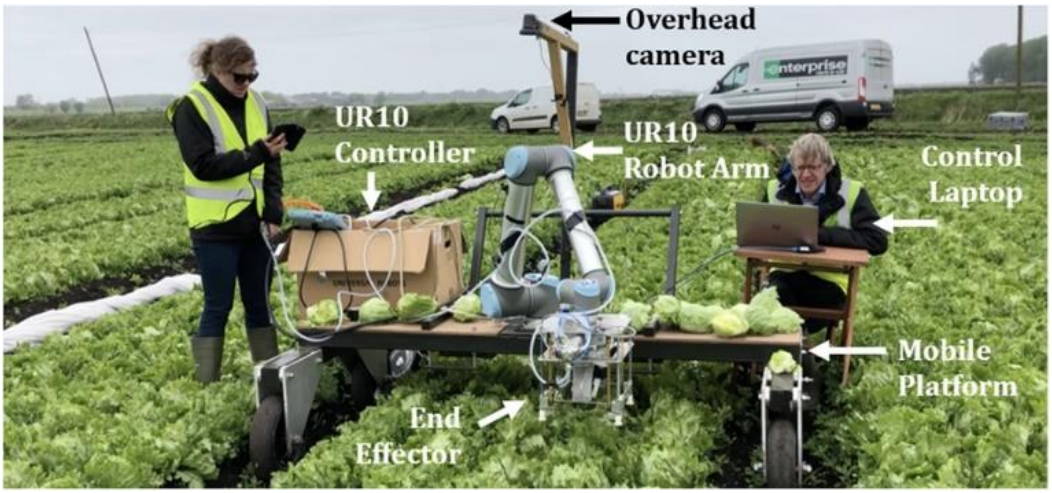

Image 7. Vegebot harvesting system
source: Birrell et al. (2019)

Harvesting is another area where robotics can benefit greenhouse growers. Birrell et al. (2019) developed a robotic harvesting system for iceberg lettuce that could autonomously navigate the greenhouse, detect and locate mature lettuce heads, and perform harvesting operations [Image 7]. Similarly, Rajalakshmi et al. (2021) developed a small-scale Cartesian coordinate farming robot that could detect and remove weeds using deep learning techniques.

2.3. Related technologies

2.3.1. Visible spectrum, Infrared spectrum and NDVI

RGB (Red Green Blue) is a tri-chromatic color model that represents colors within the visible spectrum. It is based on the human eye's sensitivity to red, green, and blue light, which are combined in various proportions to create a wide range of colors. RGB is widely used in digital imaging, displays, and color printing.

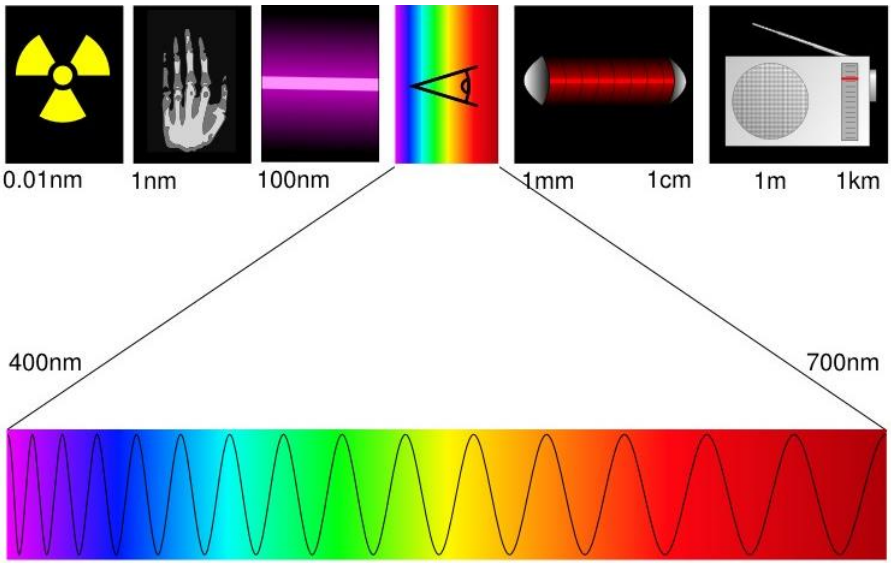

Figure 4. Visible spectrum
(Source: electricalfun.com)

In contrast, NIR (Near InfraRed) radiation is a form of electromagnetic radiation that falls outside the range of the visible spectrum, and thus belongs to the invisible spectrum.

The visible spectrum [Figure 4] is the range of colors that can be detected by the human eye. It consists of electromagnetic radiation with wavelengths ranging from approximately 400 to 700 nanometers (nm). The visible spectrum is commonly represented as a rainbow, with violet having the shortest wavelength and red having the longest wavelength.

The visible spectrum is important in various fields such as photography, art, and optics. It is used in photography to capture and display the colors of the world around us, and in art to create a wide range of colors and hues. In optics, the visible spectrum is used to design lenses, prisms, and filters to control the behavior of light.

The visible spectrum is also important in the field of science, particularly in the study of light and color. Scientists use the visible spectrum to identify elements and compounds through their unique emission or absorption spectra. Additionally, the study of color vision in humans is based on the visible spectrum, which has led to a better understanding of the physiology and perception of color.

The infrared spectrum is a region of the electromagnetic spectrum that falls beyond the visible spectrum. It includes radiation with wavelengths longer than those of visible light, ranging from approximately 700 nanometers to 1 millimeter.

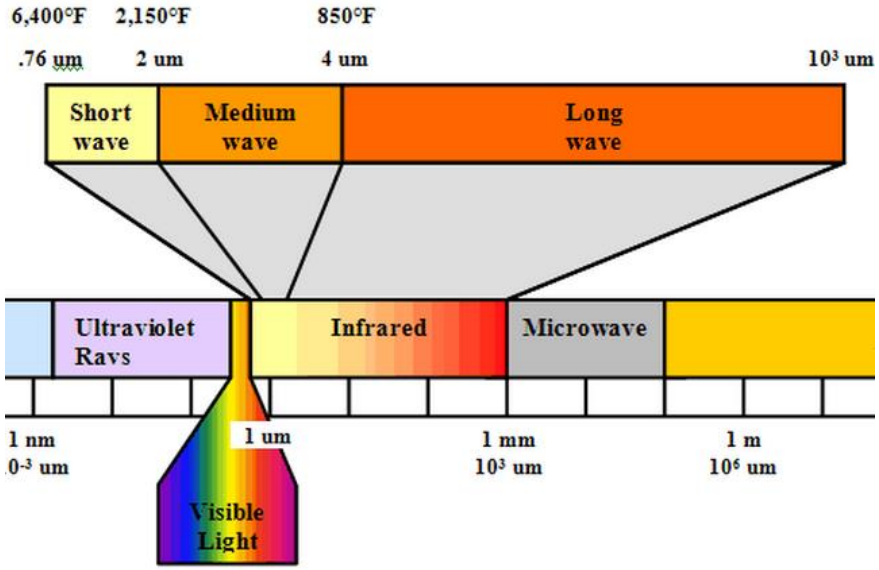

Figure 5.
Infrared spectrum (credit: Infrared Process Heating Handbook for Industrial Applications, Industrial Heating Equipment Association)

Infrared radiation is produced by the vibration and rotation of atoms and molecules, and is commonly used in various applications such as heating, communication, and imaging. The infrared spectrum [Figure 5] is divided into three main regions: near infrared (NIR), mid-infrared (MIR), and far infrared (FIR).
The NIR region, with wavelengths ranging from approximately 700 to 2500 nanometers, is used in various fields such as remote sensing, agriculture, and medicine. In remote sensing, NIR radiation is used to monitor vegetation health and soil moisture levels. In agriculture, which this thesis relates to, it can be used to assess plant health and detect stress. In medicine, NIR radiation is used for imaging and diagnostics, particularly in detecting tumors and other abnormalities.

The MIR region, with wavelengths ranging from approximately 2.5 to 50 micrometers, is commonly used for spectroscopy and material analysis. MIR radiation is absorbed by the molecular vibrations of materials, providing information about their composition and structure.

The FIR region, with wavelengths ranging from approximately 50 to 1000 micrometers, is used in various applications such as heating, sensing, and imaging. FIR radiation is absorbed by materials such as ceramics and metals, and can be used to detect and measure temperature changes.

By combining RGB and NIR photographs, it is possible to calculate NDVI, which is a commonly used vegetation index that provides valuable information about a plant's health status [Image 8 through Image 10]. NDVI is based on the difference between the amount of visible and near-infrared (NIR) radiation reflected by vegetation, and can be calculated using various remote sensing platforms, such as satellites, drones, and aircraft (NDVI, n.d.).

Image 8.
Center pivot irrigation aerial RGB image
(source: gisgeography.com)

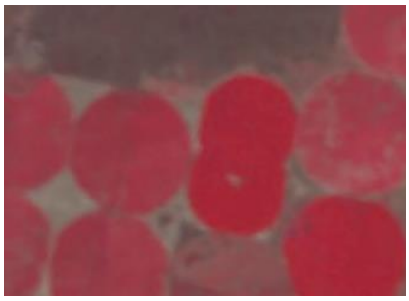

Image 9.
Center pivot irrigation aerial NIR image
(source: gisgeography.com)

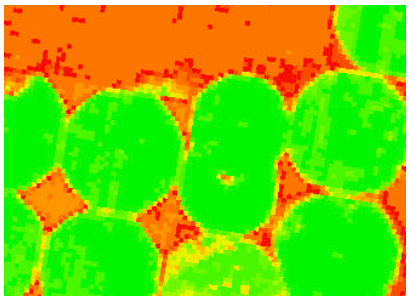

Image 10.
Center pivot irrigation aerial NDVI image
(source: gisgeography.com)

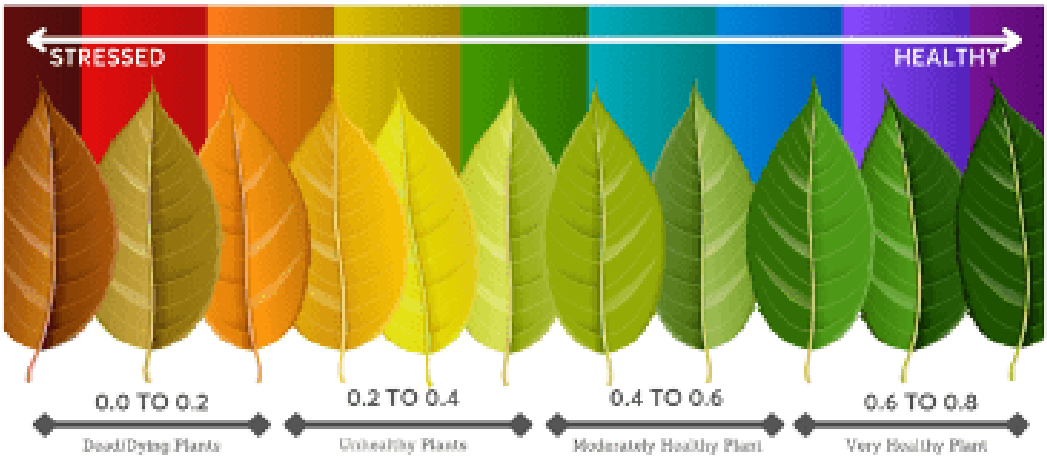

Figure 6.
NDVI Plant health (source: sentektechnologies.com)

NDVI values range from -1 to 1, with higher values indicating healthier and denser vegetation [Figure 6]. NDVI analysis is widely used in various fields, including agriculture, forestry, and ecology, as it can provide important insights into crop health, yield prediction, forest health, ecosystem productivity, and biodiversity monitoring.

The use of NDVI has become increasingly popular due to the availability of high-resolution satellite imagery and open-source software platforms such as Google Earth Engine. As such, NDVI has become a valuable tool for plant health monitoring and management, and will be discussed in greater detail in the corresponding chapter [6.3].

2.3.2. HSV color space

Identifying plants is a crucial task in agriculture and environmental research. One possible way to identify plants is by analyzing their color.

To identify plants based on their color, a picture of the plant is taken and the HSV color space is used to extract the color information from the image [Figure 7].

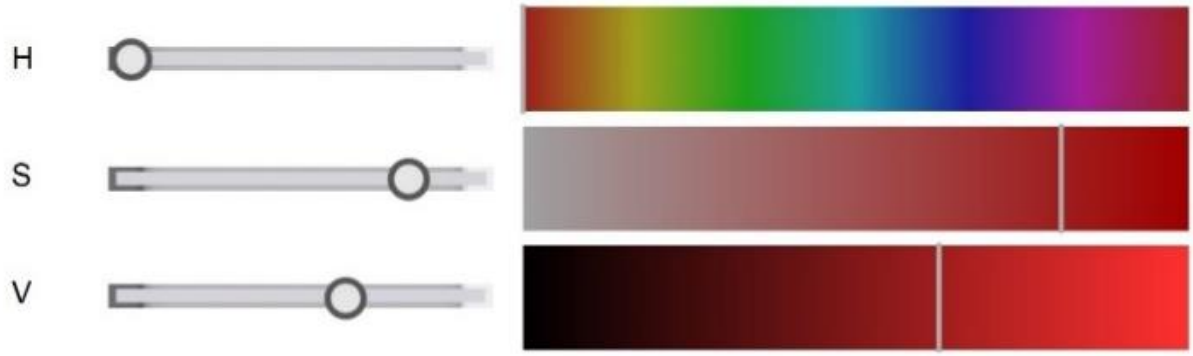

Figure 7.
HSV Color Space
source: (Hue Saturation Value (HSV) Color Space, n.d.)

HSV stands for Hue, Saturation, and Value, and it is a color space model used in color theory and image processing. In the HSV color space, colors are defined based on three dimensions:

- Hue: This represents the dominant wavelength of a color and is often represented as a color wheel. Hue values range from 0 to 360 degrees, with red at 0, green at 120, and blue at 240.
- Saturation: This measures the intensity or purity of a color. Saturation ranges from 0 to 100%, with 0% being a shade of gray and 100% being a fully saturated color.
- Value: This measures the brightness of a color. Value ranges from 0 to 100%, with 0% being black and 100% being white.

By using these three components, the HSV color space allows for more intuitive manipulation of colors, such as adjusting the brightness or saturation of an image without affecting its overall hue.
After extracting the color information from the image, a color threshold is applied to extract the pixels that belong to the plant. The threshold value is based on the color range of the plant, which can be determined by manually selecting the color range.

After extracting the plant pixels, image processing techniques such as morphological operations are used to remove noise and fill gaps in the plant regions. The plant is then encircled by the minimum enclosing circle, the center of which, is used to center the plant within the camera's field of view. This way, an RGB and an NIR picture of a perfectly centered plant is sent to the researcher.

2.3.3. Multi-exposure image fusion (MEF) to produce High Dynamic Range (HDR) images

Multi-exposure image fusion (MEF) that produces High Dynamic Range Imaging (HDR) is a technique that allows photographers and cinematographers to capture a greater range of brightness and color than is possible with traditional imaging methods, and it also has been used by Li Min (2021) to correct the color of tomato plant images. This is achieved by acquiring multiple images of the same scene with different lighting conditions or exposure times, and then combining them into a single image that simulates perfect lighting conditions.

The primary benefit of MEF is that it can help to capture scenes that have a wide range of brightness, such as sunsets, bright skies, and shadows. By taking multiple images with different exposures, MEF can combine the best aspects of each image to create a final HDR image that accurately represents the brightness and color of the scene. This can lead to more realistic and visually stunning images.

MEF is also useful for creating HDR images with greater detail in both the shadows and highlights. In traditional imaging methods, bright areas of a scene can be overexposed, resulting in loss of detail. Similarly, dark areas of a scene can be underexposed, making it difficult to see details in the shadows. By combining multiple images with different exposures, MEF can ensure that both the shadows and highlights in an HDR image have accurate and detailed information.

By acquiring multiple images with different exposures [Image 11], Multi-exposure image fusion (MEF) that produces HDR can simulate perfect lighting conditions and capture

more accurate and detailed information in both the shadows and highlights of a scene [Image 12].

Image 11.
16 images captured with different exposure times [30; 15; 8; 4; 2; 1; 1/2; 1/4; 1/8; 1/15; 1/30; 1/60; 1/120; 1/250; 1/500; 1/1000] (source: mathworks.com).

Image 12.
HDR image produced using MEF (source: mathworks.com)

This method has been explored and is discussed in greater detail in the corresponding chapter [6.2].

3. Design of the system

3.1. Requirements Analysis

The goal of this robotic arrangement is the systematic photographing of the plants of the crop in the visible and infrared spectrum for the purpose of automated monitoring of developing plants, enabling remote decision-making for plant health and plant protection [Figure 8].

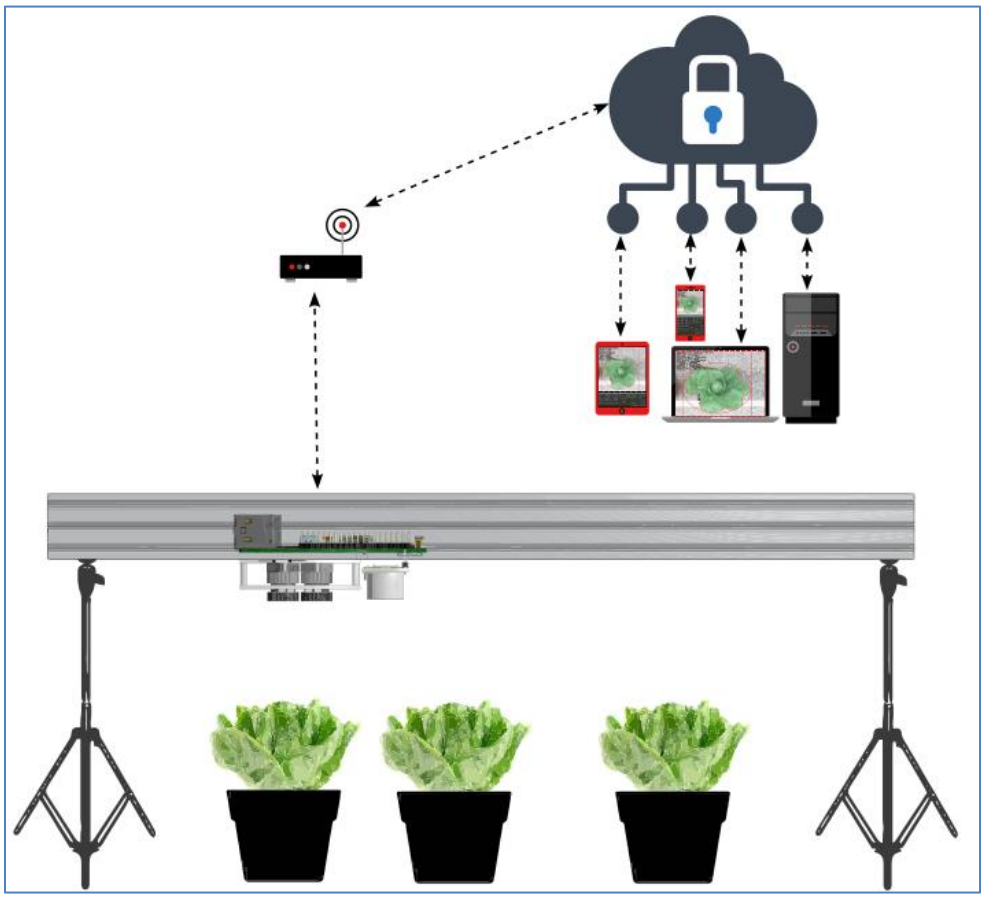

Figure 8.
Plain schematic of RoboPlantDect's layout

RGB and NIR photos of the plants are acquired and stored locally and remotely. This way, the grower can monitor the growth and health of the plants in the greenhouse without physically being present.

The device was designed according to the physical dimensions of the space available, the pots, etc. as well as the requirements of the HMU's researchers, and was named "RoboPlantDect".

The project's requirements were as follows:

- The camera must be RGB.
- The robotic camera has only one axis since it needs to monitor several lettuces in pots, placed on a 3m long – 0.4m width – 1.5m height flower pot. So, the camera must be fixed on a carriage that can be moved along an at least 3m long beam.
- The camera must be positioned above the lettuces, facing downwards.
- The structure must be lightweight and easily movable from flowerpot to flowerpot, inside the greenhouse, by two persons at most.
- The height of the structure must be adjustable so that the camera can be set to the appropriate height according to the plant's dimensions, ensuring that the camera can acquire proper images of a single plant.
- Using computer vision techniques, the lettuces must be recognized automatically.
- The lettuces must be centered within the camera's field of view and then photographed.
- The acquired images must be sent to a remote location using Wi-Fi to keep cables to a minimum of one, the 230V AC power cable.
- Controls are not needed to be implemented on the device, but a user interface is needed so that the user can operate the robotic camera. A remote desktop connection is sufficient for this. This way, the user can operate the robotic camera using a desktop computer, a tablet, a laptop or a mobile phone.
- There must be an option to manually operate the carriage with the camera.
- There must be an option to automatically monitor the plants on the flowerpot, whereby:
    - The camera starts at one end of the beam and finds the first plant.
    - The plant found is photographed, measured for its diameter, and the image is sent to a remote location.
    - The next plant is located, and the previous step is repeated.
    - The process is repeated until the last plant is found.
    - All the previous steps are repeated within a fixed time interval selected by the user, so that the growth and health of the plants are monitored.
- There must also be an infrared camera.
- Both cameras need to implement an at least 2Mpixel sensor to ensure clear images.

3.2. Design considerations

From the roof of the hydroponic greenhouse water mist nozzles are hanging. The water mist system isn't supposed to be turned on when the robotic camera is present, however, a basic water resistance was to be implemented, in case of an accidental turning on of this water mist system, or a dripping of the nozzles. Also, this eliminates the option of a robotic camera system that is hanging from the greenhouse's rooftop.

Considering the height of the flowerpots (0.7m), the height of the pots (0.27m), the height of the plants (about 0.3m) and the space between the camera and the plants (at least 0.5m), the robotic camera had to have an adjustable height of at least 1.8m, in order to be properly placed over the plants to be studied [Figure 9]. Also, the floor of the greenhouse is far from level or flat. For these reasons, a couple of photographic tripods were selected, as they are cheap, lightweight, easily adjustable, can be placed on any terrain, and depending the model, can reach a height higher than the required one.

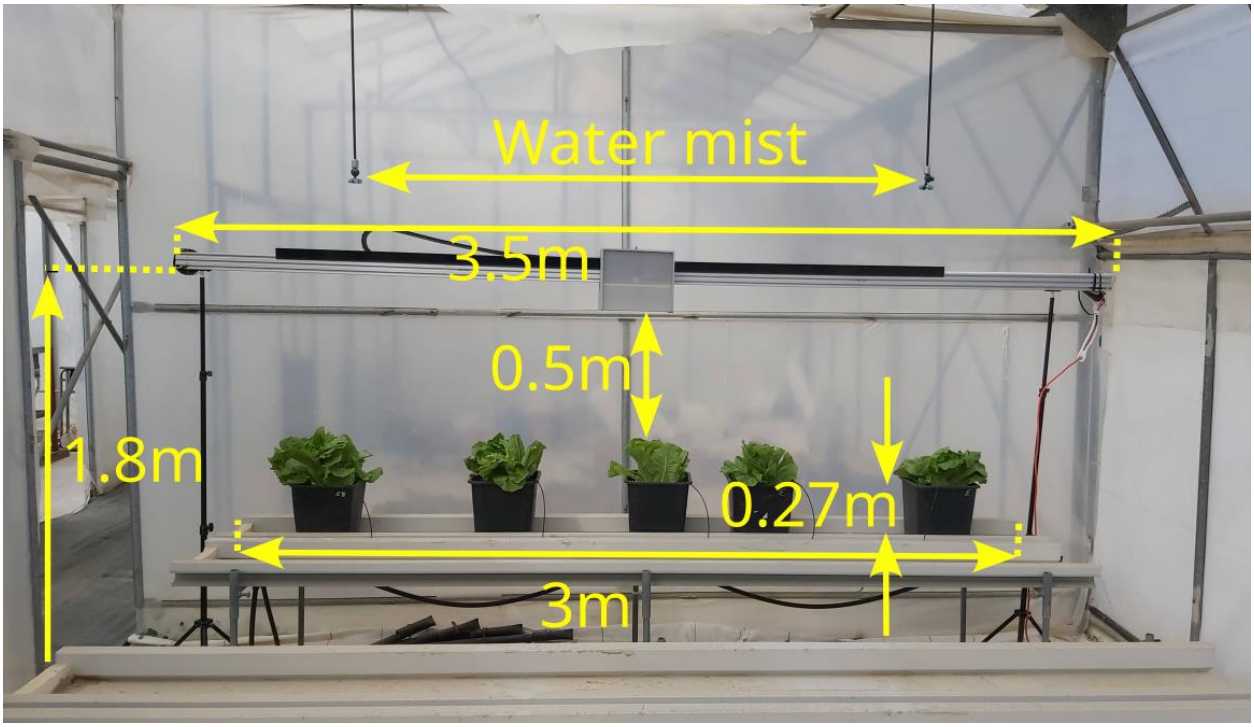

Figure 9.
Dimension requirements

The robotic structure had to be lightweight so that it can be easily moved by two persons at most, from a flowerpot, to the next one. In order to achieve this, the materials had to be lightweight, so after selecting the tripods, the aluminum beam V-Slot 2060 has been chosen. The structural properties of this beam, were found to be enough to support the carriage with all its sensors etc. without being bent significantly when reaching a length of 3.5m. The length of 3.5m was chosen in order for the tripods supporting the aluminum beam to be placed before and after the flowerpot. Such length was not to be found in the Greek market, so it was achieved by joining together a 1m, a 1.5m and a 1m beam in series, with tee nuts. Tee nuts 2020 – double M5 were the only ones to be found at the Greek market. However, tee nuts 2020 quad M5 would have performed better at securing the V-slot beams. The result proved to be not perfect, but adequately sturdy.

A desktop or a laptop computer would seriously affect the mobility of the system, so a computing system that could be powerful enough to handle machine vision routines, yet,

small and lightweight enough, had to be selected. This way, it can be embedded to the device, specifically, on the carriage. A Raspberry Pi 4 - Model B - 8GB (Rpi) has all of the properties above. Also, the embedded wifi covers the connectivity requirements. The Rpi was decided to be placed on the carriage, so that it is very close to the cameras, sensors, LEDs, stepper motor etc. and all the cables required are kept short and fixed, except the power cable which is 5m long and inserted in a drag chain of 10x10mm.

The power supplies had to be also embedded to the robotic camera, leaving only one cable to be connected to the electricity socket.

In order to measure the plant's diameter, two techniques can be used. One of them, requires a stereo camera comprised of two identical sensor-lens units. The cameras chosen do not have identical sensors, so the second technique was selected, which requires the knowledge of the camera's focal length as well as the distance between the camera's lens and the object to be measured. For this, a VL6180X ToF (Time of Flight) sensor and a HC-SR04 ultrasonic sensor were chosen in order to experiment with and choose the better one. The ToF sensor proved to be more accurate, but since the laser beam emitted is invisible, it was very difficult to determine the exact point of the measurement. Also, a fully grown lettuce's leafs can have up to 40cm difference in height. The ultrasonic sensor however, does not measure a single point, but an area, making it more suitable for measuring distances from a plant. In the end, multiple measurements were performed with both the sensors, and the mean distance was calculated, making the estimation of the plant's diameter sometimes accurate, and sometimes far from it.

Although it was not requested, a very cheap AM2301 temperature and humidity sensor was used to provide such information at the time of the photos taken. Unfortunately, reading this sensor is not always successful, so a bit of tampering with the drivers was done to repeat the process 20 times, to be –almost- certain that the sensor returns results.

A stepper motor is ideal to provide a very precise movement of the carriage. Since the aluminum beam is to be placed horizontally, the weight of the carriage is to have a minimum impact to the force needed to actually move the carriage. So, a low torque (2.8N.cm) stepper motor was selected, which proved to be rather slow, but quite adequate for the intended task. This motor was fixed on the carriage in order to keep the number of moving cables, as well as their length, to a minimum.

For adequate illumination of the plants in the visible spectrum, a 1m LED strip was fixed under the carriage. However, the NIR camera needs illumination in the infrared spectrum, so, two infrared 3W LED boards were used.

Two KW4-Z5F150 microswitches mini SPDT ON-(ON) with roller lever were used. These are ideal as limit switches. They are placed at the left and right side of the carriage in order to detect the beginning and the end of the available route.

An RGB and an infrared camera was requested, so an Arducam's stereo USB camera seemed to be an excellent choice. This consists of two cameras, a visible light (RGB) and an infrared (IR) camera. Both of them have a resolution of 2MP. The RGB one is used for the plant recognition.
The eight LEDs on the Arducam's stereo USB camera board are infrared, and they are switched on automatically when the IR camera is used.

3.3. Selection of the hardware materials

3.3.1. Metal structure and moving parts

Tripods
For the support of the structure, two camera tripods were used capable of extending up to 210cm height [Image 13].
These are very lightweight, and they offer simplicity in height adjustment. Furthermore, tripods are capable of being placed in any rough terrain, like greenhouses have.

Image 13.
Tripod

Image 14.
Tripod mounting plate

Image 15.
V-Slot 2060

Image 16.
Tee nuts 2020 – quad M5

Tripod mounting plates.
At the top of the tripods, a tripod mounting plate ¼" is placed [Image 14], in order to fit the tripods to the aluminum beams.

Aluminum beams.
For the aluminum beams, V-Slot 2060 were selected [Image 15].
V-Slot's building characteristics are much like traditional T-Slot but V-Slot then goes on to add new levels of functionality through its internal v grooves that allow for linear motion.

Image 17.
Tee nuts 2020 – double M5

Image 18.
Cable Drag Chain 10x10mm

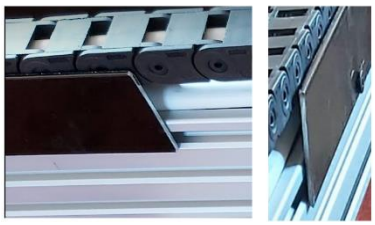

Image 19.
Aluminum beams 1x40mm

Tee nut 2020 – Double M5
For connecting the V-slot 2060 in series, tee nuts 2020 – double M5 are used [Image 17].
The same tee nuts are used to secure the timing belt on the V-slot 2060 beams.
However, tee nuts 2020 quad M5 [Image 16] are recommended for extra securing force of the V-slot beams.
Unfortunately, at the time of the making, these were not available at the Greek market.

Cable Drag Chain 10x10mm
On top of the V-slot 2060 beams, a Cable Drag Chain 10x10mm is placed [Image 18], to provide the correct support and movement of the power cable.
Made of nylon, with bending radius 18mm and outside dimensions 17x14mm, they are ideal for the intended application.

Aluminum beams 1x40mm
In order for the cable drag chain to stay on top of the V-slot 2060 beams (and not fall off at either side), 2 1x40mm aluminum beams were cut, drilled and are used as walls [Image 19].

Tee Nut 2020 – Spring Loaded M5

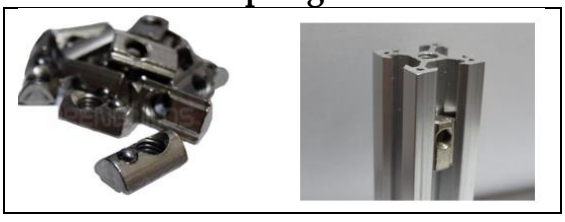

Image 20.
Tee Nut 2020 - Spring Loaded M5

Image 21.
V-Slot Gantry Set 2020x2080 Xtreme

Image 22.
NEMA 17 Stepper Motor

The latter aluminum beams, were secured with Tee Nuts 2020 - Spring Loaded M5 [Image 20].
The spring loaded ball prevents unwanted movement of the nut in the slot. This allows for inserting nuts in the vertical position as they will not slide from gravity.

3.3.2. Movement transmission

V-Slot Gantry Set 2020x2080 Xtreme
As a carriage this V-slot Gantry set is used [Image 21]. It proved to be very versatile, sturdy and reliable.

Stepper motor
A high-torque stepper motor in size NEMA 17 (42 mm) with 1.8° step angle (full step) with D-Shaft for easy and reliable connection with coupler, is used [Image 22].
This is a bipolar motor made by Wantai Motors, with a part number 42BYGHW208P1-X5.

Aluminum GT2 Timing Pulley - 12T - 5mm Bore
On the stepper motor, an Aluminum GT2 Timing Pulley - 12T - 5mm Bore [Image 23] is fixed.
This pulley has 12 teeth, and a 5mm inner bore. Two set screws can be used to attach it firmly to any 5mm diameter shaft such as one of our stepper motors. Full aluminum construction means these are very light and very durable.
Its small diameter retains the torque produced by the stepper motor.

Timing Belt - GT2
A 5m long, GT2 timing belt [Image 24] is used for movement transmission.

Image 23. Aluminum GT2 Timing Pulley - 12T - 5mm Bore

Image 24. GT2 timing belt

Image 25. AM2301 Temperature and Humidity sensor

Image 26. VL53L0X ToF distance sensor

3.3.3. Sensors

Digital Temperature & Humidity Sensor
This AM2301 temperature and humidity sensor [Image 25] is a basic, low-cost digital temperature and humidity sensor.
It uses a capacitive humidity sensor and a thermistor to measure the surrounding air, and returns a digital signal on the data pin (no analog input pins needed).

Distance Sensors
A VL53L0X is used [Image 26]. The sensor contains a tiny invisible laser source, and a matching sensor. The VL53L0X can detect the "Time of Flight", or how long the light has taken to bounce back to the sensor. Since it uses a very narrow light source, it is good for determining distance of only the surface directly in front of it. Unlike sonars that bounce ultrasonic waves, the 'cone' of sensing is very narrow. Unlike IR distance sensors that try to measure the amount of light bounced, the VL53L0x is much more precise and doesn't have linearity problems or 'double imaging' where you can't tell if an object is very far or very close.
This distance sensor, proved to be very accurate, but the angle of detection is too narrow for the case of fully grown lettuces. The height of a lettuce can vary from just a few cm at the side leaves, to 40cm at the center. Thus another sensor was used as well, with a much wider angle of detection (30 degrees), in order to achieve the measuring of the mean height of the lettuce.

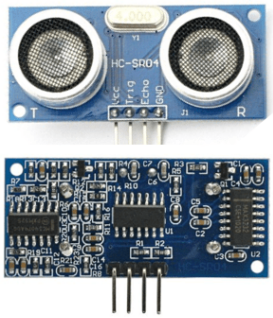

Image 27. HC-SR04 ultrasonic sensor

Image 28. Infrared LED Board

Image 29. LED Strip

Image 30. Power Supply 12V 2A

The HC-SR04 ultrasonic sensor [Image 27] uses a sonar to determine the distance to an object. This sensor reads from 2cm to 400cm with an accuracy of 0.3cm.

3.3.4. Illumination

Infrared LED Board
A couple of Infrared LED Boards were utilized for proper infrared illumination [Image 28]. The onboard adjustable resistor is set to allow the LED to turn on in any ambient light conditions.

LED Strip SMD3528 5V
It is made of 60 3528 LED's per meter and the input voltage is 5VDC [Image 29]. The USB connector was removed.

3.3.5. Power Supplies

Power Supply 12VDC 2A PSU-1602
A 12VDC 2A PSU-1602 power supply [Image 30] is used for powering the stepper motor and the cooling fan, and it can handle both devices easily.
The output connector was removed, since it was not needed.

Power Supply 5.1V 3A - Raspberry Pi 4 Official

Image 31. Power Supply 5.1V 3Ax

Image 32. KW4-Z5F150 micro switch

Image 33. In-line switch

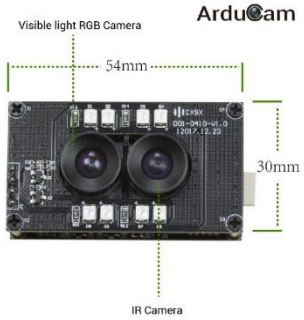

Image 34. Arducam's stereo USB camera

The official Raspberry Pi USB-C power supply [Image 31] is used to power the latest Raspberry Pi 4 Model B. This is a high quality power supply, capable of powering the Rpi and all the peripherals.

3.3.6. Switches

Microswitches
A couple of KW4-Z5F150 micro switch mini SPDT ON-(ON) with roller lever [Image 32] were utilized in order to determine the start and end of the carriage's available route.

Power switch
In order to facilitate the control of two power supplies, an in-line switch [Image 33] has been employed downstream of the power supplies, resulting in the interruption of the round cable. This configuration allows for the operation of both power supplies to be regulated by a singular switch.

3.3.7. Cameras

Dual USB Camera
For plant identification an Arducam's stereo USB camera was utilized [Image 34]. It utilizes an RGB and a NIR camera, both of them are 2 Megapixels.

8MP Motorized Zoom Camera

Image 35. Arducam's 8MP motorized zoom

Image 36. Raspberry Pi 4 8GB

Image 37. Heatsinks

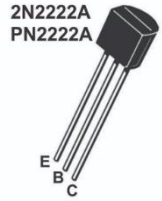

Image 38. 2N2222A

Image 39. JST connectors

2MP might be enough for plant detection, but 8MP can produce a lot more detailed images. An Arducam's 8MP motorized zoom camera [Image 35] is used in conjunction with the other ones. It's motorized zoom and focus capabilities are utilized to get the best possible images.

3.3.8. Computational Unit

It has been decided that the carriage movement, as well as the image acquisition, processing and storage will be controlled by one computing unit, small enough to fit on the carriage, and powerful enough to perform the needed tasks.
The Raspberry Pi 4 - Model B - 8GB [Image 36] is ideal, since it supports Wifi, embeds USB ports and has sufficient computing power and 8GB RAM to process the acquired images.
However, considering the elevated temperatures that can be reached inside a greenhouse, for cooling the Raspberry Pi heatsinks [Image 37] were used in conjunction with a 12V fan.

3.3.9. Electronic components

For controlling the fan, the LEDs, the infrared LEDs and the relay that controls the stepper motor driver, 2N2222A NPN transistors were used [Image 38], which are capable of handling the current needed for these devices.
For connecting all the devices with the PCB, JST XH 2.5mm connectors [Image 39] proved to be ideal for the task.

3.4. Software tools

3.4.1. OpenCV

In this thesis, the use of OpenCV (OpenCV, n.d.) for identifying plants based on their color has been chosen.

OpenCV (Open Source Computer Vision) is an open-source computer vision and machine learning software library that provides developers with a wide range of tools for real-time image and video processing. It was initially developed by Intel in 1999, but since then, it has been maintained and developed by a community of developers.

OpenCV supports a wide range of programming languages such as C++, Python, Java, and MATLAB, making it highly accessible to developers across various platforms. The library provides numerous built-in functions that allow developers to perform various image and video processing tasks such as image filtering, feature detection, object recognition, and tracking, among others.

The library has applications in various fields, including robotics, biometrics, surveillance, and automotive, among others. Its popularity can be attributed to its robustness, reliability, and ease of use, which make it an ideal choice for real-time image and video processing applications. OpenCV is widely used in industry and academia, and its continuous development and community support make it an excellent choice for image and video processing tasks.

3.4.2. Syncthing continuous file synchronization

To facilitate efficient acquisition of files by the user, a file synchronization program called Syncthing (Syncthing, n.d.) has been chosen.

Syncthing is a free, open-source, decentralized file synchronization tool that utilizes a peer-to-peer (P2P) network to sync files securely and privately across multiple devices. The tool was created as an alternative to traditional cloud-based synchronization solutions that rely on a central server to synchronize files.

The decentralization of Syncthing is a fundamental feature that distinguishes it from other synchronization tools. In a P2P network, all devices are treated as equals, and each device runs its own instance of Syncthing. Files are synchronized directly between devices without passing through a central server, which ensures that users have full control over their data and can keep it private.
The security of Syncthing is also a critical aspect of the tool. Syncthing uses industry-standard encryption to protect files in transit and at rest. Communication between

devices is encrypted using TLS, and files are encrypted with AES-256 before being sent over the network. The tool also supports device authentication, which allows users to ensure that only trusted devices can access their files.

In addition to its security features, Syncthing is highly customizable, allowing users to configure the tool to meet their specific needs. Users can choose which folders to sync, set bandwidth limits, and define synchronization rules. Syncthing also includes a web-based user interface that makes it easy to manage devices and monitor synchronization status.

Overall, Syncthing is a powerful tool that offers a free, flexible and secure way to sync files across multiple devices, thus, an excellent choice for RoboPlantDect.

3.4.3. Remote Desktop Software

A remote desktop application is a software tool that enables a user to remotely access and control another computer or device over a network or the internet. This type of application allows a user to view and interact with the desktop, files, and applications on the remote computer as if they were sitting in front of it.

To save space and reduce clutter, RoboPlantDect has not any display, mouse or keyboard connected to the Raspberry Pi, thus, a remote desktop application had to be installed.

In order to ensure that the system can be used even if the remote desktop servers are offline, not one, but two were installed to the Rpi.

- VNC® Server (VNC® Server, n.d.)
- AnyDesk (AnyDesk, n.d.)

Both of them offer non-paid versions. They have been tested and used, and both of them proved to be perfect for the job.

The user must install either VNC® Viewer (VNC® Viewer, n.d.) or AnyDesk to his/her terminal and connect to the account that has been created for the needs of RoboPlantDect. If needed, the account can be changed. Then, provided that RoboPlantDect is connected to the internet, RoboPlantDect will be shown to VNC® Viewer or AnyDesk and the user can connect to it and use it from anywhere in the world.
It is worth mentioning that both of these remote desktop applications can be used simultaneously, allowing more than one users to connect to RoboPlantDect at once, if needed.

4. Implementation of the System

4.1. Schematic and PCB

In order to connect all the required devices and electronic components, an appropriate circuit [Figure 10] and PCB [Image 40] was designed using a powerful online PCB design tool called EasyEDA (EasyEDA, n.d.).

For the simplicity of the PCB implementation, a one sided PCB board was used, as the other side has only two lines, which were replaced with a couple of cable bridges.

Future component utilization was taken into account. This way, more components can be added in the future, thus, making the system highly customizable. In fact, HC-SR04 ultrasonic sensor was easily added after the whole system was implemented.

The PCB was implemented and all the components were assembled and soldered [Image 41].

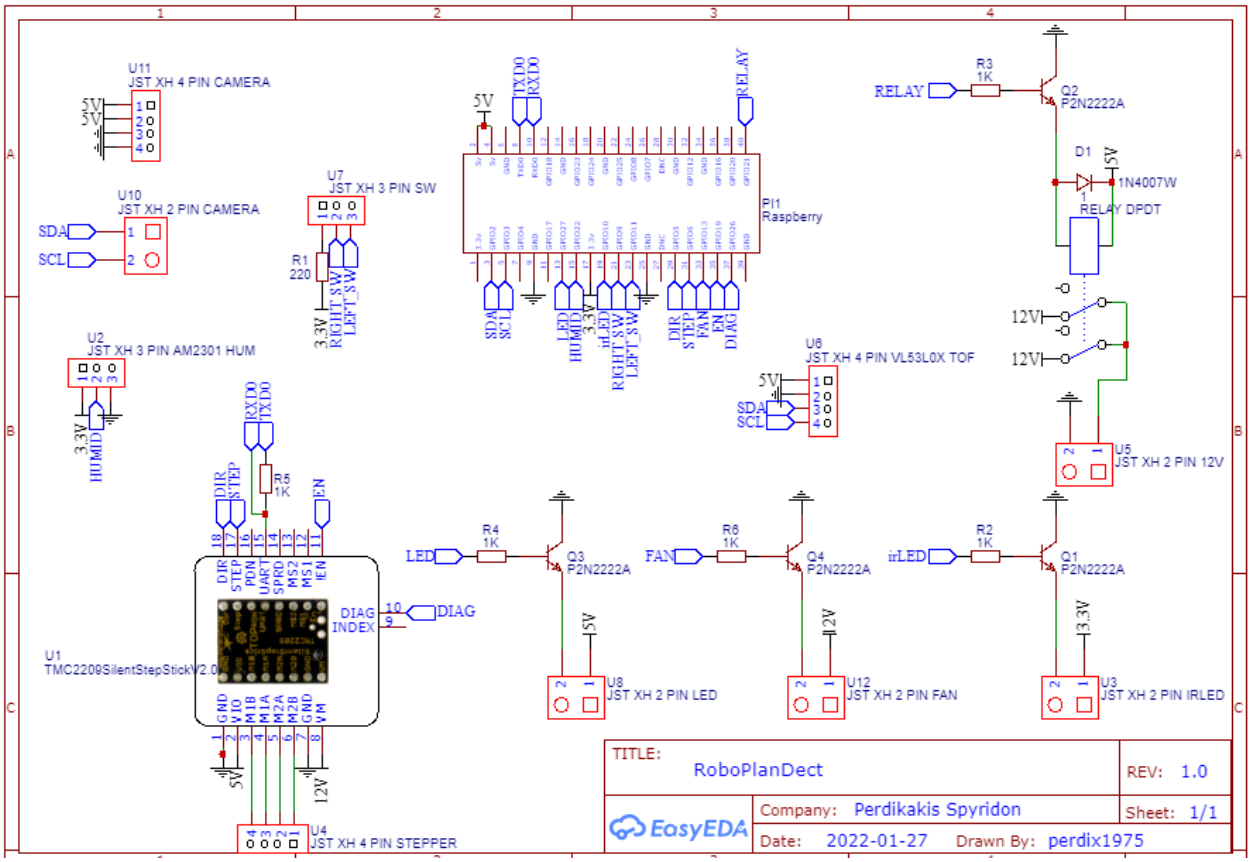

Figure 10.
RoboPlantDect Schematic

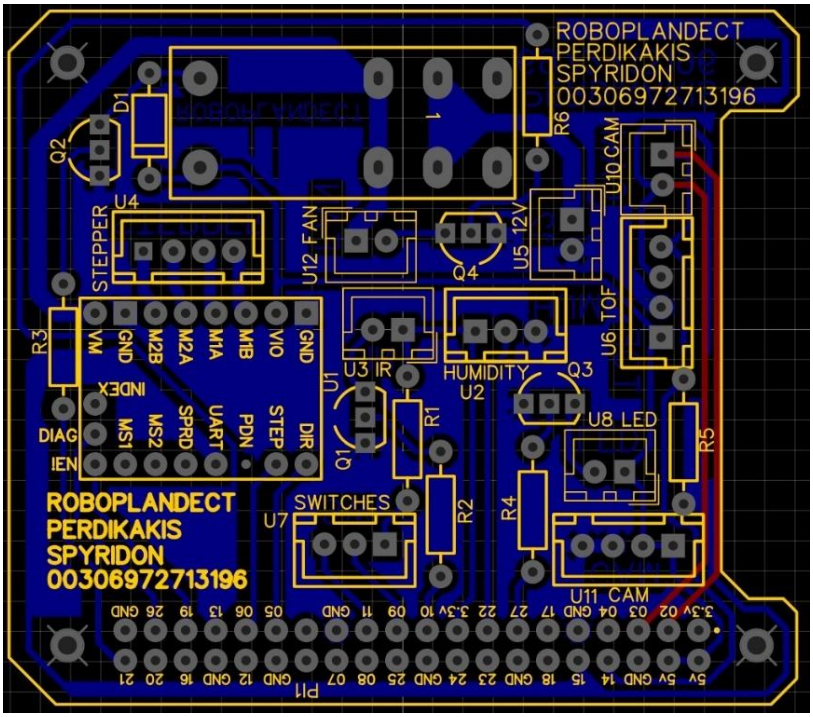

Image 40.
RoboPlantDect PCB

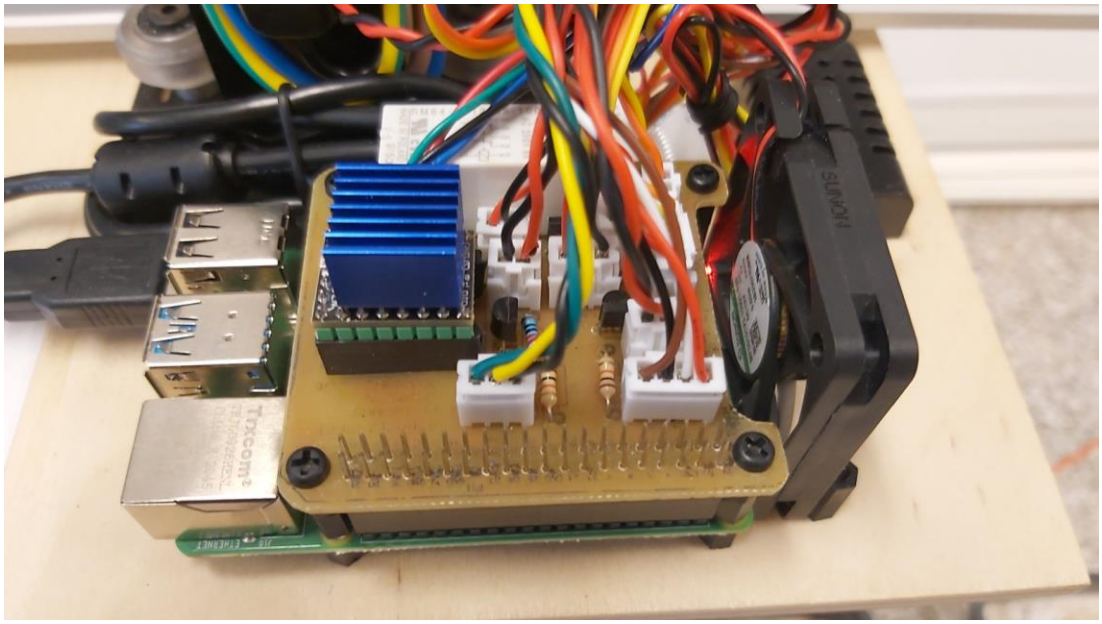

Image 41.
RoboPlantDect PCB assembled.

4.2. Hardware assembly

4.2.1. System description

Three V-Slot 2060 aluminum beams were connected in series, one 1.5m and two 1m long, thus, the desired 3.5m were achieved. By placing the 60mm side vertically, no bending is observed through all 3.5 meters.

At the edges of the 3.5m beam, the two tripods are attached to support the whole structure.

Image 42.
RoboPlantDect Assembled in the Lab

A carriage is made using the V-Slot Gantry Set 2020x2080 Xtreme, under which, a 250 x 150 x 6mm plywood is secured.

Under the plywood carriage, the distance sensor, the LED strip, the infrared LEDs, the microswitches, the cameras are placed, facing downwards.

The stepper motor is also placed under the carriage, but it's shaft is facing upwards, in order to connect with the timing belt.

The microswitches are placed at the far right and far left end of the carriage respectively. When the carriage reaches the end of the route, the corresponding microswitch is making contact with the tripod. This way, the system determines the beginning and the end of the available route on the beam.

The timing belt is placed through all the length of the beam, and it is fixed at the two ends of the beam. This timing belt is 5m long, but was not trimmed to the 3.5m of the aluminum

beam. This enables the option to add another 1.5m aluminum beam, having a total effective route of 5m, if needed.

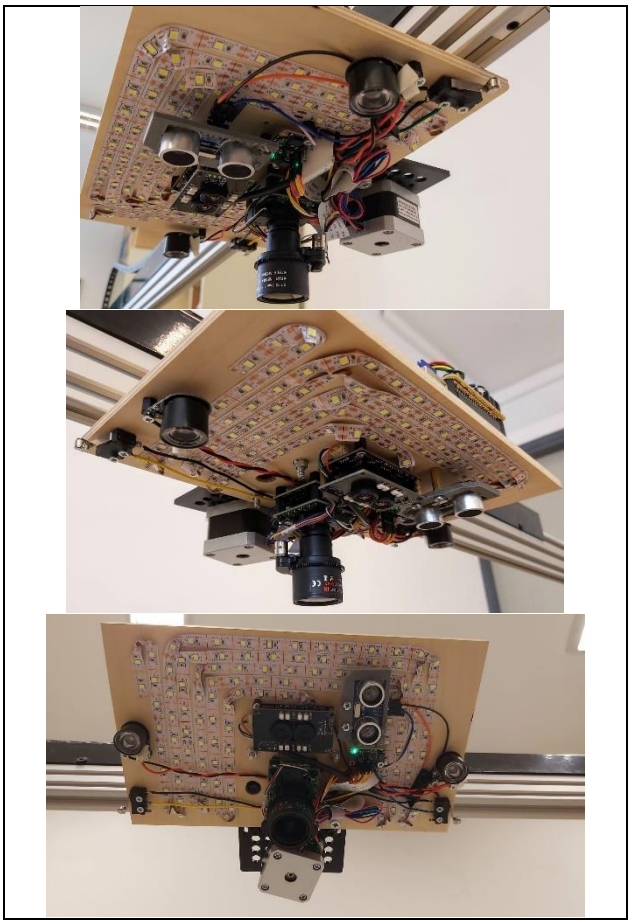

Image 44.
LEDs, sensors cameras and switches

Image 43.
Plywood box

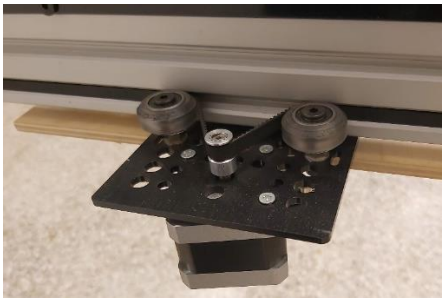

Image 45.
Carriage movement layout

The Aluminum GT2 Timing Pulley - 16T - 5mm Bore is fixed on the stepper motor shaft and the timing belt is connected with it.

On the carriage, the Raspberry Pi, the PCB, the fan and the temperature and humidity sensor are placed.

On the beam, the Cable Drag Chain 10x10mm is placed, to provide the correct support and movement of the YDY 3 x 2.5mm^2 power cable. One of the cables is used for the positive of the 5.1VDC power supply. The second cable is used for the positive of the 12VDC power supply. The last cable is used as ground for both power supplies.

In order for the cable drag chain to stay on top of the V-slot 2060 beams (and not fall off at either side), 2 1x40mm aluminum beams were cut, drilled and are used as sidewalls.

On the carriage, a 35x115x20mm plywood beam is fixed, in order to link the carriage with the drag chain and cable. On this beam, the power switch is secured.

In order to protect the carriage -and all the components on it- from accidental use of the greenhouse's mist watering system, a water resistant plywood box has been designed [Image 43].

All the cameras, sensors, LEDs and switches are secured under the carriage [Image 44].

The assembled system can be shown in [Image 42].

4.2.2. Movement of the robotic system

The movement of the carriage is performed by one 12V, 0.4A/phase, 200 steps/revolution stepper motor. For this purpose, a high-torque stepper motor in size NEMA17 (42 mm) with 1.8° step angle (full step) with D-Shaft, for easy and reliable connection with a coupler, was used. The stepper motor placed under the carriage, but its shaft is facing upwards, in order to connect with the timing belt, and all together form a linear traveler drive system [Image 45]. On the stepper motor, an Aluminum GT2 Timing Pulley - 12T - 5mm Bore was fixed. This pulley has 12 teeth, and a 5mm inner bore. Two set of screws can be further used to attach it firmly to any 5mm diameter shaft such as the one used in our stepper motor. Its small diameter retains the torque produced by the stepper motor. A 3.5m long, GT2-type timing belt (2mm Pitch, 6mm width, made of Neoprene and Fiberglass materials) was fastened at the two ends of the 3.5m long beam and used for movement transmission. As the axis of the stepper motor rotates, the timing pulley forces the carriage to move across the beam.

The stepper motor's control was achieved by one TMC2209 V2.0 stepper motor driver, connected to the raspberry pi and using a microstepping factor of 2, resulting in 400 steps per revolution of the motor's shaft.
The calculated steps per mm for the linear motion produced with the belt, was found to be 16.667 steps/mm [Equation 1], where $S_{rev} = 200steps$ is the number of steps per revolution of the motor, $f_m = 2$ is the microstepping factor, $p = 2mm$ is the pitch and $N_t = 12$ is the number of the attached to the motor's shaft pulley's teeth.

$$\frac{steps}{mm} = \frac{S_{rev} f_{mp}}{pN_t} = \frac{200 * 2}{2 * 12} = \frac{400}{24} = 16.667$$

Equation 1.
Steps per millimeter

4.3. Software Development

4.3.1. User Interface

RoboPlantDect is equipped with an intuitive and relatively lightweight user interface (UI) [Image 46], developed using cvui (cvui 2.7.0, n.d.) that is built on top of OpenCV drawing primitives and where the user can perform a considerable number of tasks.

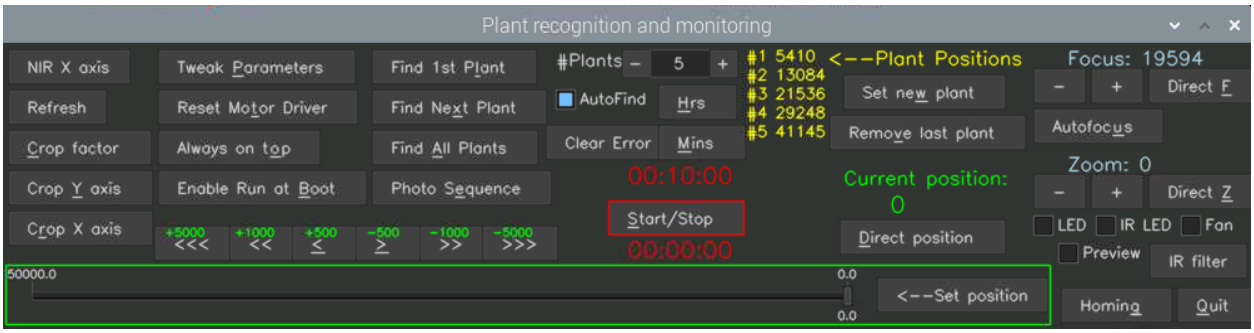

Image 46.
User Interface

There are various buttons and indicators, whose functions are briefly explained:

- **NIR X axis**: The difference in steps between the RGB and NIR cameras.
- **Refresh**: Refreshes the image in the current position.
- **Crop factor**: The percentage of the total RGB image that is cropped.
- **Crop Y axis**: The percentage of the RGB image that is cropped on the Y axis.
- **Crop X axis**: The percentage of the RGB image that is cropped on the X axis.
- **Tweak Parameters**: The operation of this button is thoroughly described at a previous chapter
- **Reset Motor Driver**: Restart of the stepper motor driver. Use this button if the carriage's movement is erratic! This behavior is extremely rare, however, it has been observed.
- **Always on top**: Makes the user interface window always on top.
- **Enable Run at Boot**: With system startup, the program runs automatically so that in case of temporary power outage, the programmed processes can continue normally.
- **Find 1st Plant**: Locates the first plant that exists.
- **Find Next Plant**: Locates the next plant in order. The carriage will first move forward as many steps as JumpSteps is set at.
- **Find All Plants**: Locates all available plants.
- **Photo Sequence**: Immediate start of the photo taking process.
- **#Plants**: The number of plants that need to be located.

- **AutoFind**: If enabled, then during the Photo Sequence process, plants will be recognized automatically or not.
- **Clear Error**: In case the system detects fewer plants than the number declared in the #Plants field, then there is an error, and the LEDs flash to notify the user. This button cancels the error.
- **Hrs**: Hours in the Photo Sequence recurring process.
- **Mins**: Minutes in the Photo Sequence recurring process.
- **Start**/Stop: Start/cancel the recurring Photo Sequence process.
- **Plant positions**: A list of the positions of the located plants in steps.
- **Set new plant**: Manually add a new plant to the end of the plant position list, in steps.
- **Remove last plant**: Remove the last plant from the plant position list.
- **Current position**: The current position of the carriage in steps.
- **Direct position**: Moving the carriage to a new position, in steps.
- **Set position**: Moving the carriage to the position defined by the slider located at the bottom of the user interface, in steps.
- **Focus**: The position of the motorized focus of the 8MP camera.
    - **-** : Decrease the position of the motorized focus of the 8MP camera.
    - **+**: Increase the position of the motorized focus of the 8MP camera.
    - **Direct F**: Directly control the motorized focus of the 8MP camera by setting the desired number.
- **Autofocus**: Automatic focus of the 8MP camera.
- **Zoom**: The position of the motorized zoom of the 8MP camera.
    - **-** : Decrease the position of the motorized zoom of the 8MP camera.
    - **+**: Increase the position of the motorized zoom of the 8MP camera.
    - **Direct Z**: Directly control the motorized zoom of the 8MP camera by setting the desired number.
- **LED**: Direct control of the visible LED strip.
- **IR LED**: Direct control of the infrared LEDs.
- **FAN**: Direct control of the cooling fan.
- **Preview**: Display the current image from the 8MP camera.
- **IR filter**: Toggle engagement of the 8MP camera's infrared filter.
- **Homing**: Locate the zero position of the carriage. Please wait until the process is completed.
- **Quit**: Exit the program.

4.3.2. System Initialization

General Approach

In order to facilitate optimal utilization of the software, the user must conscientiously execute a series of mandatory and discretionary actions, as elucidated in Figure 11.

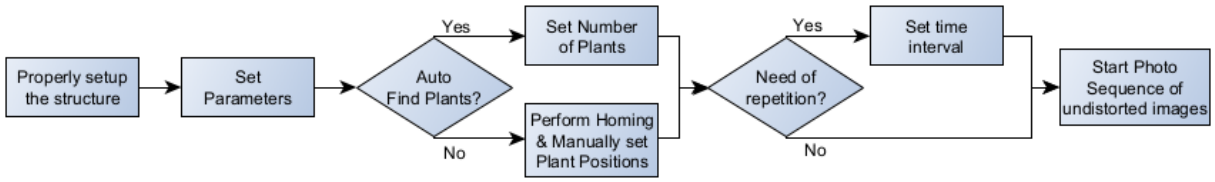

Figure 11.
Actions required from the user

The foremost obligatory action entails the judicious configuration of the structure. Specifically, the aluminum beam must be positioned parallel to the flowerpot and, as the carriage moves, the camera must be positioned in precise alignment with the plants to be monitored. The user must also take into account the dynamic growth of the plants, necessitating the estimation of the optimal distance between the camera and the mature plant. Furthermore, the user must establish a wireless connection between the Raspberry Pi and the Wi-Fi network, which may mandate the use of an Ethernet cable in the initial phase, for remote access to the Raspberry Pi's desktop, and subsequently, for the setup of the Wi-Fi connection. The Ethernet cable is rendered redundant in the subsequent phases.

The subsequent step entails the meticulous configuration of all essential parameters to facilitate the effective operation of the system, as described in chapter [4.3.2].

Following this, the user must deliberate on whether the system is to detect the plants automatically or manually. In the former scenario, the user must explicitly specify the number of plants that the system is expected to detect. In contrast, in the latter scenario, the user must perform a homing of the carriage to ascertain the starting position, and subsequently, enter the position of each plant manually.

Moreover, the user must deliberate on whether the plants are to be photographed repetitively. If this is the case, the user must specify the optimal time interval for each photo sequence and commence the timer. Conversely, in the absence of such a requirement, the user may initiate the photo sequence immediately, and it will be performed only once. It is important to consider the distortion that occurs due to the camera's lens, as discussed in chapter [4.3.2] In order to obtain accurate and reliable images for analysis, image undistortion is applied to correct for any lens distortion that is present. This can help to ensure that the images accurately represent the plants and their growth over time.

The software has been developed to support all of the above requirements, providing users with a highly efficient and effective means of analyzing plants.

Parameterization of the system

After the RoboPlantDect's structure has been established, the user is required to configure the various parameters of the system, which include:

- **Crop Factor**.
  The RGB camera is the one utilized to detect the plants to be photographed. This camera produces 1920x1080 images having a wide field of view, which can provide a lot more information than the wanted plant.
  The crop factor is a parameter that symmetrically crops the acquired images in both x and y-axis. It is as if the user zooms in or out of the image, but no actual zooming is happening, only cropping.
  According to the plant's dimensional properties, a cropped photo can:
    - Set to adequately include the plant (e.g. a square photo for a lettuce)
    - Exclude unneeded areas of the camera's available field of view.
    - Keep the size of the photo small.
    - Reduce the processing time.
- **Crop Y axis**.
  The user is required to choose the number of pixels to crop the image produced by the RGB camera along the Y axis, effectively shifting the image vertically.
- **Crop X axis**.
  The user is required to select the number of pixels for cropping the produced image of the RGB camera along the X-axis. This parameter is used to shift the image either towards the left or towards the right.

Pushing the "Tweak Parameters" button, three windows appear, consecutively:

- Set the **maximum position** in steps.
  The system is designed so that the length of the available route that the carriage follows, can be lengthened or shortened, by moving the position of the tripods along the aluminum beam, or/and by adding or subtracting aluminum beams. Thus, the maximum position of the carriage must be set manually. If the user makes a mistake and sets a value of the position that the carriage cannot go to, then a physical switch will be triggered at the end of the route, and the actual maximum position will be set automatically.
- **Jump Steps**.
  Upon locating a plant, the image carriage undergoes a motion in order to align the plant at the center of the captured image. In order to locate the next plant, the previously detected plant must be disregarded and left behind, otherwise the same plant may be detected repeatedly. The user inputs the number of carriage steps required to move away from the current plant in order to locate the next one. This value is subject to variation based on the physical dimensions of the plant, as well as the camera's distance from the plant. The user must also exercise caution in selecting this value not to be too high, to ensure that the subsequent plant is not overlooked.

- **Color picker**.
  The user can manually set the positions of the plants, however, there is an automated process of setting the plants' positions. The system recognizes each plant, aligns the center of the camera to the plant and stores its position. The recognition of the plant is based on its color. In order to achieve this, the "Color Picker" window was implemented [Image 47], where the user must move the sliders to carefully choose the correct upper and lower thresholds of Hue, Saturation and Value [Image 48] in order to keep only the colors of the plant. All the other colors are filtered out of the image, thus keeping only the plant and a black background [Image 49].

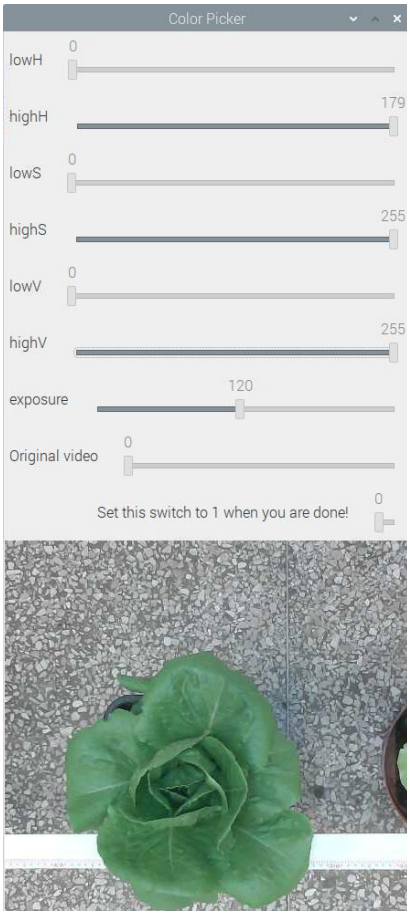

Image 47.
Color Picker:
Colors not suppressed

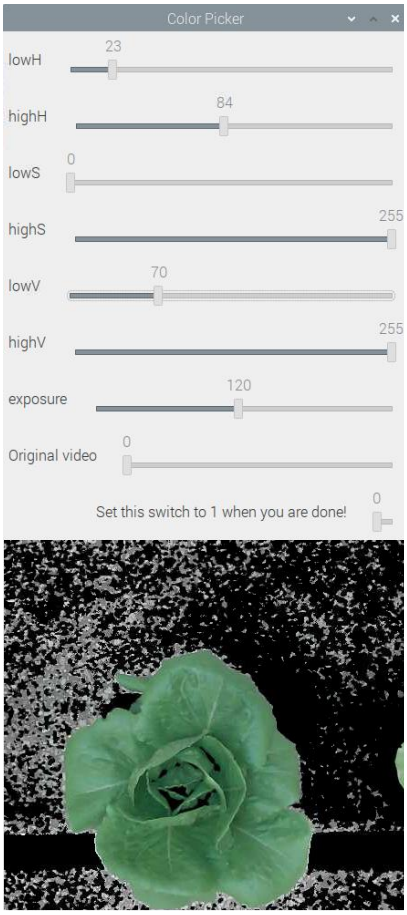

Image 48.
Color Picker:
Hue, Value are adjusted

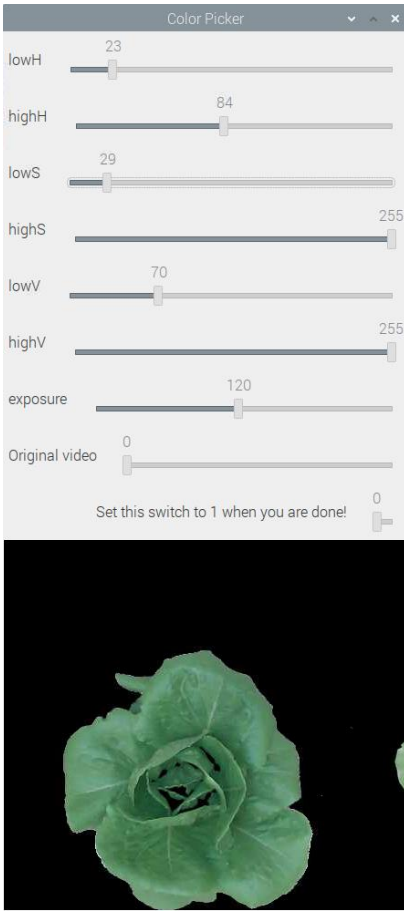

Image 49.
Color Picker:
Saturation also adjusted

Depending on the lighting conditions the value of "exposure" slider must be selected. Below the sliders, a real time video is being projected for the user's convenience. When the "Original video" switch is set to 0, the video shows in real time what the program sees after setting the sliders, excluding a range of colors. To close the window "Color Picker" and save the settings, the user must set the corresponding switch to 1.

Homing

In order to initiate RoboPlantDect, the precise location of the image carriage must be established. To accomplish this, a switch is utilized, which serves as a homing limit switch [Image 50].

Initially, the carriage is commanded to move -600000 steps from its current position, which translates to a displacement of $600000 steps / 16.667 mm = 36 m$. This ensures that the carriage reaches the starting point of the available route.

Image 50.
Limit Switch

Upon arriving at the start of the route, the homing limit switch is triggered by colliding with the tripod, which causes it to transition from an open to a closed state.

This event then triggers a callback (interrupt) that immediately halts the stepper motor and consecutively advances the carriage by 60 steps, causing the homing limit switch to transition back to its original state.
The new position of the carriage is then set as the 0 position.

Upon reaching an appropriate distance from its initial position, the carriage attains its ultimate velocity, which may result in a variance of up to 1 millimeter between the actual 0 position setting of consecutive homing processes.
By executing the homing procedure twice in succession, the positional variance is nullified, ensuring that the 0 position remains consistent.

This is attributed to the fact that the distance traveled during the second homing process is infinitesimal, and the stepper motor is programmed to gradually accelerate prior to attaining its maximum velocity, thereby sustaining a very low actual speed, which ultimately leads to a more consistent actual 0 position.

It is crucial to meticulously verify that no impediments exist in the path of the carriage, as this may impede the homing limit switch from colliding with the tripod. This unfortunate eventuality can lead to the stepper motor attempting to traverse the distance of 36 meters while simultaneously skipping steps, resulting in erroneous homing outcomes that cannot be trusted.

Subsequent to any motion of the carriage, the precise position of the carriage is stored in a designated file, to guarantee that in the event of a subsequent program execution, the carriage's position is automatically retrieved from that file. If the user can confidently ascertain that the carriage has not undergone any displacement in the intervening period, then the mandatory homing procedure can be circumvented, thereby expediting the execution of the procedures.

Timer for repeated plant recognition and acquisition

A significant function of the system is setting the scheduled interval of repeating the plant recognition and image acquisition process, as well as the number of the plants to be identified. In short, repeatedly, the system:

- Executes a homing procedure, to determine the starting point of the carriage.
- If AutoFind button is checked, the system identifies the plants and records their exact position.
- The carriage is placed to the recorded positions, and the system acquires images of the plants, taken from the RGB, NIR and 8MP cameras respectively and records the plant's distance from the cameras, according to the distance sensor's readings.
- Processes the images acquired by the RGB camera in order to determine each plant's contours, its diameter and center, its surface area as well as its mass center.

Image 51.
Timer

- Records the date and time and in combination with the calculated data values reported previously, performs data logging of all these data, to a log file. The same information are superimposed on each image, however, the original images are kept as well. Finally, saves locally the acquired RGB and NIR images in distinct folders.
- The folders of the images and all data recorded, are automatically synchronized with other PCs through the cloud.

The timer stands out in the user interface as the red color coded section [Image 51].

Lens distortion correction

The phenomenon of lens distortion is a prevalent issue in the fields of photography and computer vision, where straight lines in the real world appear curved or bent in the captured image. This problem arises due to the optical properties of the lens, such as its material and shape, leading to the deformation of the images and causing them to appear stretched or distorted. The distorted images can prove to be problematic in applications where precision and accuracy are crucial, such as robotics, autonomous vehicles, and object recognition.

OpenCV offers a comprehensive suite of tools for manipulating images and videos, including functions for correcting lens distortion, which can rectify the distorted images and restore them to their original, undistorted state (OpenDV Camera Calibration, n.d.). The correction process involves determining the distortion parameters of the lens and applying a correction algorithm to the image.

One of the most commonly used methods of correcting lens distortion in OpenCV is the utilization of calibration patterns, such as checkerboards, to estimate the distortion parameters. This technique involves placing the calibration pattern within the camera's field of view and taking multiple images at different angles and distances. These images are then processed using OpenCV functions to identify the calibration pattern and calculate the lens distortion parameters, which can be stored and utilized to rectify any image captured by the same lens.

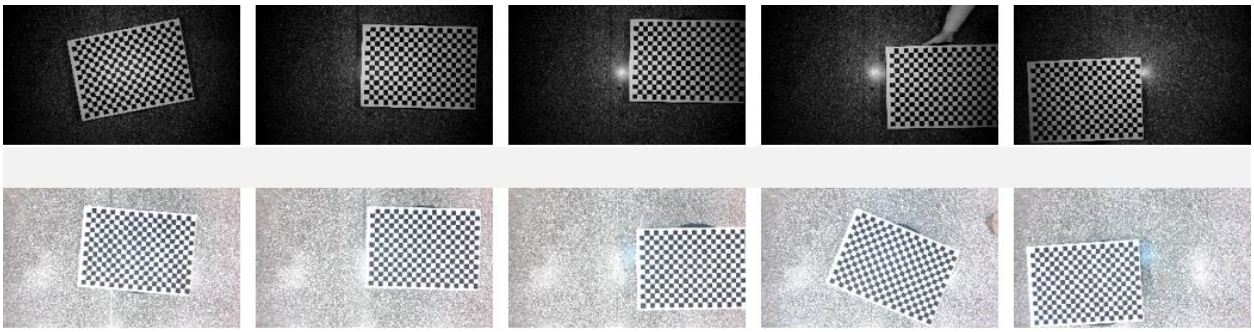

Image 52.
Checkerboards for calibrating NIR and RGB cameras

A sequence of images was captured, depicting a printed 23X16 squares checkerboard, at various angles and positions of the visible area of both NIR and RGB cameras. These images [Image 52] were used to calculate the 3x3 camera intrinsic matrix, along with the translation and rotation of each image, which were utilized to correct the distortion of the captured images of the plants.

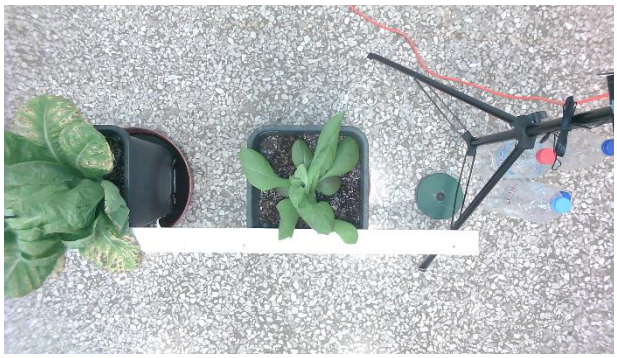

Image 53.
RGB original picture

Image 54.
RGB undistorted picture

Image 55.
NIR original picture

Image 56.
NIR undistorted picture

The original and undistorted images of the plants can be visualized in images [Image 53 through Image 56]. The results show that although the lenses of both NIR and RGB cameras were of the same type manufactured by the same company, the NIR camera's lens induced significantly less distortion to the image than the RGB's.

Although the distortion in the center area of the images from both cameras is minimal, rendering the undistortion process impractical for calculating the plant's area and size, the images acquired from the RGB or NIR cameras are automatically undistorted based on the camera's specific distortion parameters, even if it is not explicitly mentioned in the block diagrams.

4.3.3. Image acquisition, Plant identification & Localization

In brief, the system operates as follows:
- The system first identifies the plants and records their precise location.
- It then acquires images of the plants, captured by both the RGB and NIR cameras, and measures the plant's distance from the cameras using data from the distance sensors.

- The system then processes the images to determine each plant's contours, diameter, center, surface area, and mass center.
- All data collected, including the date and time of acquisition and the data values computed earlier, are logged to a file. The same information is superimposed on each image while preserving the original images. The system also saves the acquired RGB and NIR images in separate folders.
-The image folders and all recorded data are then synchronized with other PCs via the cloud.

To locate the plants for further study, the following procedures are carried out [Figure 12]:

- The first essential procedure involves moving the carriage to position 0. This position is at the far right of the available route.
- The user selects the number of plants to identify, and a plant counter is set accordingly, determining the number of procedural loops to execute.
- The RGB camera is used to detect the plants and is initialized.
- An image is captured and immediately undistorted for processing [Image 57, Image 58].
- This particular RGB camera has a very wide field of view, so the image is cropped [Image 59] to ensure that only one plant (and possibly small segments of other plants) is present in the image. This also ensures that there will be less processing time for the smaller image.
- A Gaussian blur is applied to the image using the GaussianBlur() function to filter out high-frequency noise.
- In order to work with HSV Color Space which is needed, the image is converted to this color space.
- The user has preselected upper and lower thresholds for Hue, Saturation, and Value, which are used to identify the color of the plants. In this procedure, using function inRange(), undesirable colors are masked out leaving black space [Image 60].
- Using functions erode() and dilate(), a series of erosion and dilation operations are performed to make the plants more solid and distinguishable, in case small blobs appear in the images.
- The findContours() function of OpenCV is used to determine the objects found in the image.
- If no objects are found, the process is repeated from the top, after shifting the carriage slightly to the left, as many steps as the user has previously set as Jump Steps.

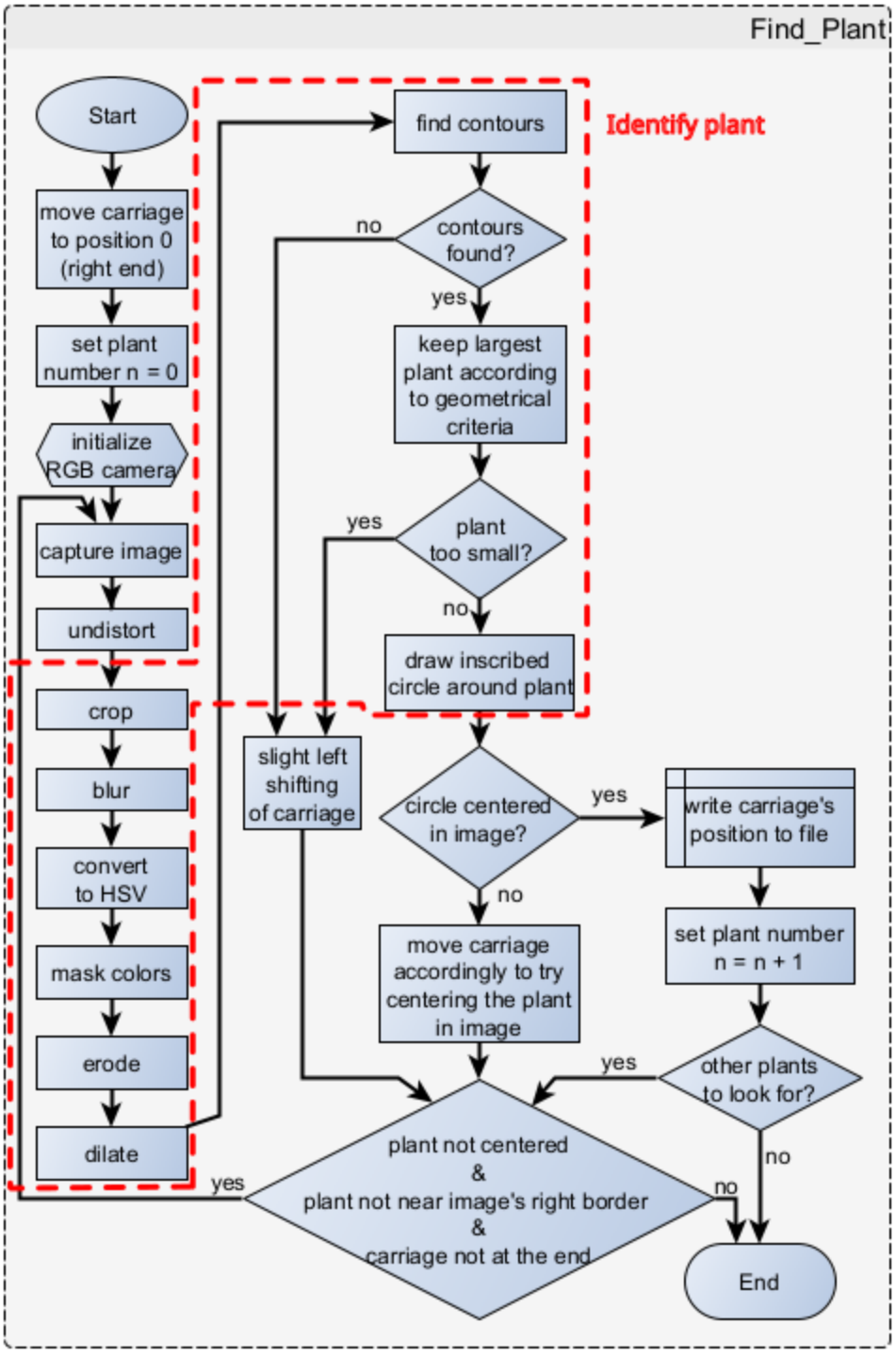

Figure 12.
Find_Plant function

- If more than one contours are found [Image 61], then after applying the function contourArea() of OpenCV, and the function max(), the smaller ones are discarded, thus keeping the largest one [Image 62].

- If the contour found is considered to be too small to be a plant, then once again, the process is repeated from the top, after shifting slightly the carriage to the left (2000 steps).
- After determining a contour that can be a plant, the minEnclosingCircle() function is applied to the contour. This function returns the coordinates of the circle's center and radius, in order to draw an inscribed circle around the plant [Image 63].
- If the center of the plant isn't in the center of the image, then the carriage is shifted to the left or right accordingly, in order to bring the camera exactly on top of the plant. Then the whole process is repeated from the top. Otherwise, the carriage's position (thus, the plant's position) is recorded to a file and the plant counter is incremented by one.
- If there are no other plants to look for, the procedure has come to an end.

Image 57.
The original image from RGB camera

Image 58.
RGB Undistorted

Image 59.
RGB Cropped

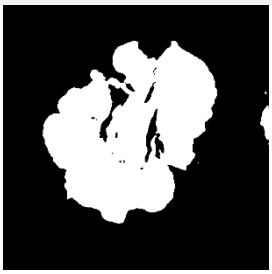

Image 60.
RGB Masked

Image 61. RGB Masked + Cropped

Image 62. RGB Largest Plant

Image 63.
RGB Circled

Image 64. RGB Embedded Info

Image 65.
8MP Camera

Image 66. 8MP Camera without IR filter

Image 67.
The original image from NIR camera

Image 68.
NIR Undistorted

Image 69.
NIR Cropped

After the plant recognition and the recording of their positions, a number of steps are taken in order to obtain the photos of the plants and process the data acquired from the various sensors [Figure 13].

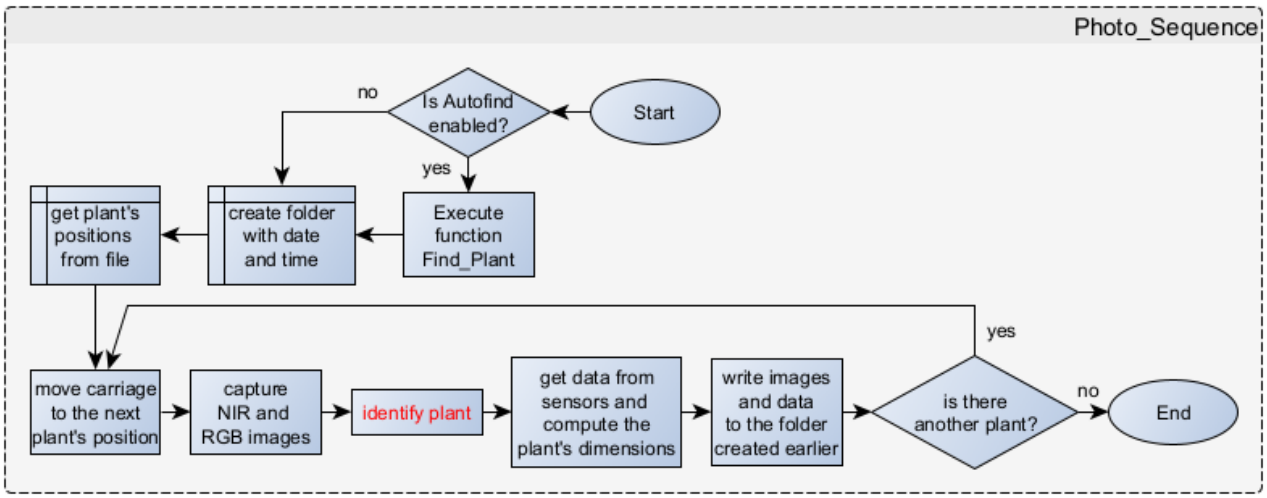

Figure 13.
Photo_Sequence Function

- If checkbox Autofind is enabled, then the function Find_Plant() is executed, in order to find the plants' location, prior to the final images acquisition - photography.
- A folder is created and named according to the current date and time.
- The plant's positions are read from the relevant file.
- The carriage is moved to the next plant's position.
- NIR and RGB images are captured from the stereo camera and 8MP camera [Image 65 through Image 69], after moving the carriage to the appropriate position, in order that all images are captured from the exact same spot.
- Within the RGB image, the plant is identified. Contour, center of mass, center of the plant, surface area of the plant, as well as other info are computed.

- The carriage is once again moved in various positions near the plant's center, in order to obtain multiple measurements from the distance sensors. The mean distance of the plant to the camera is then calculated.
- Various images (original, cropped, with [Image 64] and without calculated data) are written into the folder created earlier [Image 57 through Image 69].
- The whole process is repeated until all the available plants have been processed.

The determination of a plant's width using a camera and a distance sensor, requires fundamental mathematical computations, specifically, the application of the equation governing similar triangles for equal and opposite angles (scantips Calculate Distance or Size of an Object in a photo image, n.d.). This equation is directly applicable in this case, as depicted in [Figure 14].

$$\frac{P}{f} = \frac{D}{L} \Leftrightarrow \boldsymbol{D = \frac{PL}{f}}$$

Equation 2. Plant's actual width

In [Equation 2]:
P = Plant's width on sensor (mm)
f = focal length of the camera (mm)
D = Plant's actual width (mm)
L = Plant's distance from the camera's sensor

The camera's manufacturer specifies the focal length to be:
f = 3mm ±5%.
OpenCV enables the determination of the plant's diameter in pixels. Furthermore, the manufacturer specifies that each pixel measures 3x3 micrometers. Thus, the plant's width on the camera sensor in millimeters can be expressed as:

P = Plant's width in pixels * 0.003(mm)

However, determining the distance L from the plant to the camera's sensor is challenging due to the plant's morphology, which causes variations in its height across its width. To overcome this challenge, two sensors were utilized: an HC-SR04 ultrasonic sensor and a VL53L0X Time of Flight (ToF) sensor.

The ToF sensor offers a narrow sensing cone, ensuring high accuracy in distance measurements. Nevertheless, the laser used is not visible, resulting in uncertainty regarding which point of the plant is being measured. In contrast, the HC-SR04 ultrasonic sensor possesses a 30-degree angle of detection (manufacturer specifies an effective angle of less than 15°). The ultrasonic sensor appears to be more suited for measuring plant distances, but unfortunately, the sensor used frequently yields excessively large and unrealistic results. To overcome this issue, the function distanceUltrasonic() was developed, returning the median of 30 measurements.

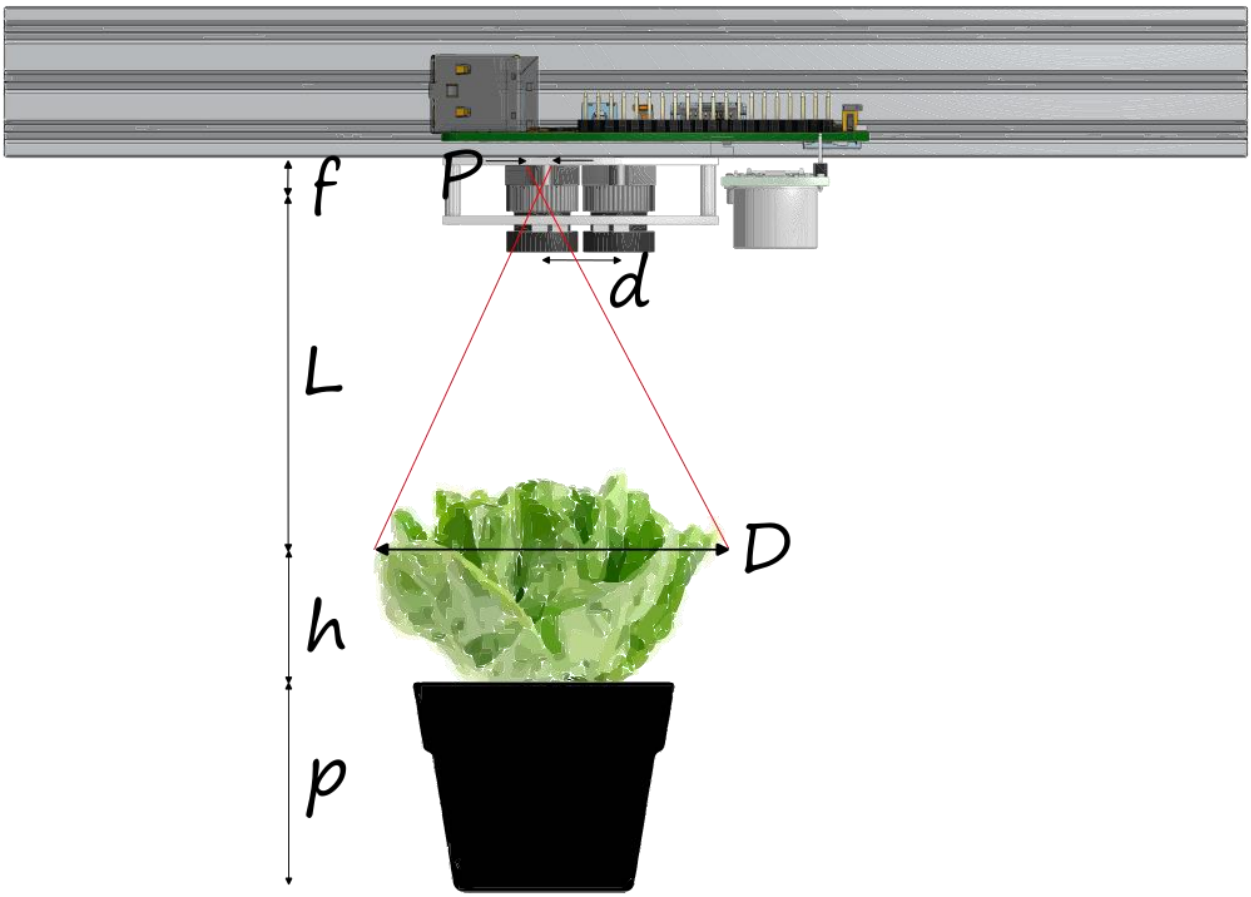

Figure 14.
Plant's width calculation

After a series of measurements using both sensors, it was decided to employ both distance sensors. The sensors make three measurements each, one directly above the plant's center, and two others two centimeters to the right and left of it. The mean of these measurements is taken as the final distance L from the plant.

Obviously, this method can't be perfect in accuracy. To address this issue, in the image, the detected plant is circled with a minimal enclosing circle, and two vertical red lines are drawn [Image 70]. Using these two lines in conjunction with the tape measure, the researcher can visually calculate the diameter of the plant.

In this particular image, one can see that the left vertical line is at 57.3cm of the measuring tape, and the right one is at 88.8cm. The subtraction gives a diameter of 31.5cm. The system has automatically calculated a diameter of 30.3cm, which is only a 3.88% percentage difference [Equation 3].

$$\left| \frac{31.5 - 30.3}{\frac{31.5 + 30.3}{2}} \right| * 100\% = 3.88\%$$

Equation 3.
% difference between the auto and manual diameter measurement

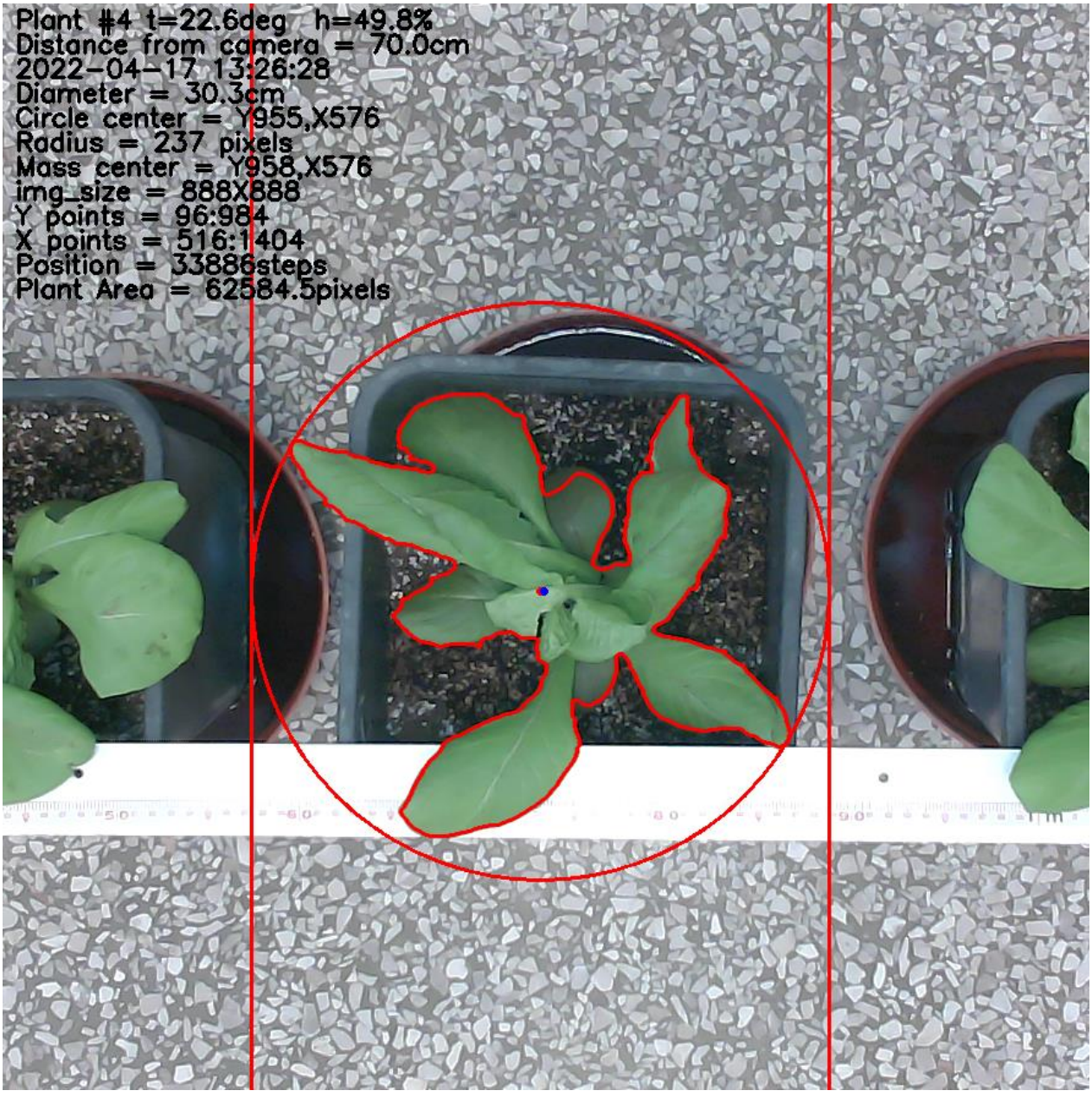

Image 70.
Detected plant with various info embedded in the picture

Other information are embedded in the image for the user's convenience:

- The number of the plant of the particular photo sequence.
- The temperature t and humidity h at the time of the capturing.
- The calculated distance from the camera.
- The date and time.
- The calculated diameter of the plant.
- The center of the minimum enclosing circle (also shown as a red dot).
- The radius of the minimum enclosing circle in pixels.
- The exact position of the plant's mass center (also shown as a blue dot) in the original image that hasn't been cropped.
- The size of this image which depends upon the zoom factor etc.
- The X and Y points of the original image that correspond to this cropped one.
- The position of the carriage in steps.
- The plant's area in pixels.

5. Evaluation of the system

5.1. Precision of movement

The aluminum beam that supports the camera and the carriage has been assembled from two 1.5-meter pieces and one 1-meter piece, creating two joints that can slightly alter the angle of the carriage during movement.

This structural weakness can, in turn, cause the center of the camera's field of view to shift unpredictably.

Additionally, when the aluminum beams are supported by two tripods with a distance of 3.5 meters between them, a slight bending of the beam is expected to occur.

In order to evaluate the accuracy and repeatability of the carriage's movement, an experiment was planned and executed [Image 71].

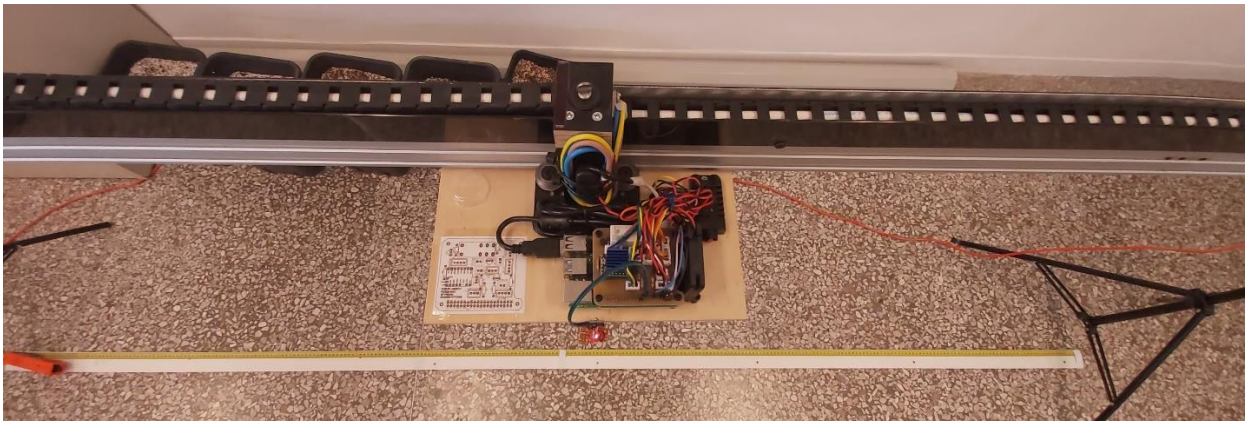

Image 71.
Setup for determining the precision of movement

The aluminum beam of the structure was set at a height of 1 meter above the ground, and a red dot laser pointer was mounted on the carriage [Image 72], facing downwards. A measure tape was placed parallel to the aluminum beam on the floor, allowing the red laser dot to point at the tape [Image 73].

This setup allowed for accurate measurement of the difference between the calculated theoretical position of the camera's center of view and its actual position.

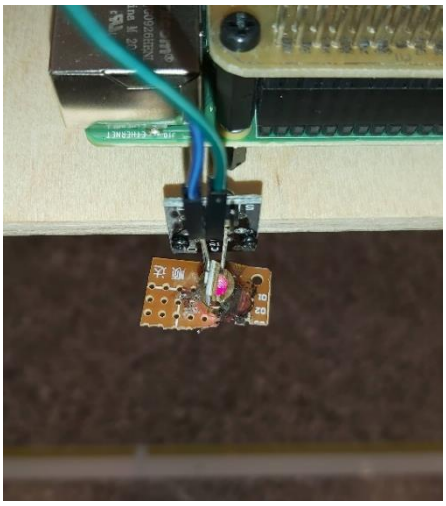

Image 72.
The red dot laser pointer

The experiment involved a series of movement commands to specific points, with the carriage set to move to 15 different points in steps of the stepper motor. The actual position of the red dot on the measuring tape was recorded for each movement, and the distance between the expected target's center and the actual center was then calculated. The entire process was repeated 10 times, and the mean distance and standard deviation were calculated and recorded in a table.

Image 73.
The red dot on the measuring tape

Despite the structural flaws inherent in the system, the results of the experiment were excellent in terms of the accuracy and repeatability of the carriage's movement. The mean error was kept between 0 and 1.65 millimeters, and the standard deviation was kept between 0 and 0.26 millimeters. These results demonstrate that the RoboPlantDect system is highly reliable and can provide accurate and consistent results even in the presence of structural weaknesses.
A series of movement to a specific point commands was iterated.

The carriage was set to move to 15 specific points (in steps of the stepper motor), and the actual position of the red dot on the measuring tape was recorded.
The distance between the expected target's center and the actual center, was then calculated.

The whole process was repeated 10 times, and the results of the mean distance (Mean) and standard deviation (STD) was calculated and shown in table [Table 1].

Target	Steps	Absolute distance from "home" in X-axis (mm)	Calculated distance from the expected target's center (mm)											
			Experiment's iteration										Mean	STD
			1	2	3	4	5	6	7	8	9	10		
1	0	0	0	0	0	0	0	0	0	0	0	0	**0**	**0**
2	1667	100.02	0.02	0.02	0.02	0.02	0.02	0.02	0.02	0.02	0.02	0.02	**0.02**	**0**
3	5000	300	0	0	0	0	0	0	0	0	0	0	**0**	**0**
4	6500	390	0.5	0.5	0.5	0.5	0.5	0.5	0.5	0.5	0.5	0.5	**0.5**	**0**
5	11000	660	1	1	0.5	1	0.5	1	0.5	1	0.5	1	**0.8**	**0.26**
6	15000	900	1.5	1.5	1.5	1.5	1	1.5	1.5	1.5	1.5	1.5	**1.45**	**0.16**
7	19000	1140	1.5	1.5	2	2	2	1.5	1.5	1.5	1.5	1.5	**1.65**	**0.24**
8	22000	1320	1	1.5	1	1.5	1	1	1	1	1	1	**1.1**	**0.21**
9	26000	1560	1	1	1	1	1	1	1	1	1	1	**1**	**0**
10	30000	1800	0.5	0.5	0.5	0.5	0.5	0.5	0.5	0.5	0.5	0.5	**0.5**	**0**
11	33000	1980	0.5	0	0.5	0	0	0.5	0.5	0.5	0	0.5	**0.3**	**0.26**
12	38000	2280	0	0	0	0	0	0	0	0	0	0	**0**	**0**
13	43000	2580	1.5	1.5	1.5	1.5	1.5	1.5	1.5	1.5	1.5	1.5	**1.5**	**0**
14	46000	2760	1	1.5	1	1.5	1.5	1.5	1.5	1.5	1	1.5	**1.35**	**0.24**
15	50000	3000	1	1	1	1	1	1	1	1	1	1	**1**	**0**

Table 1. Accuracy and repeatability of carriage's movement

The mean error is kept between 0 and 1.65mm, and the standard deviation is kept between 0 and 0.26mm, which indicates that despite the structural flaws, the system behaves excellent in terms of the accuracy and repeatability of the carriage's movement.

5.2. Plant Identification Precision

In order to evaluate the accuracy of plant identification, an experiment was planned and executed at the lab.

The aluminum beam of the structure was set at a height of 1 meter above the ground, and under it, pots with lettuces [Image 74]. A total of 43 lettuces were automatically identified, traced, measured [Image 75] and photographed by RoboPlantDect.

Image 74.
Top view of the system, monitoring an array of lettuces

All of these lettuces were also manually traced [Image 76] using the open source scientific multidimensional image processing program ImageJ (ImageJ, n.d.) and the minimum enclosing circle's center, as well as the plant's mass center were calculated.

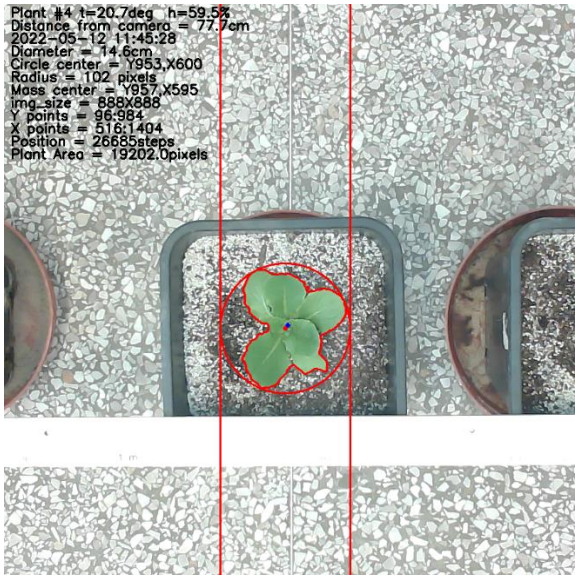

Image 75.
Auto plant identification

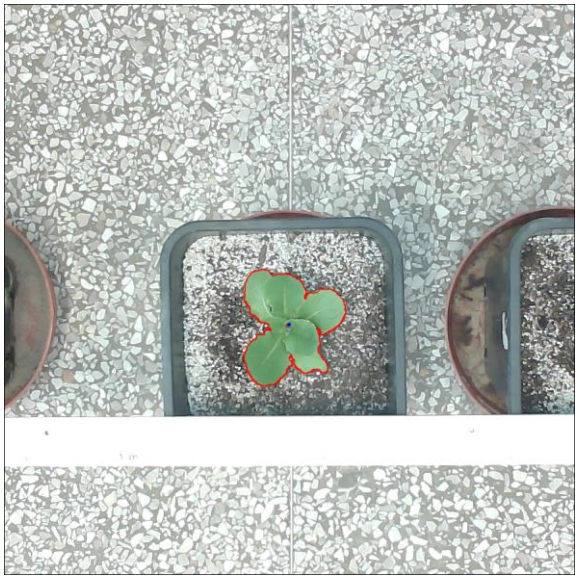

Image 76.
Manual tracing and measurement

The distance between the circle and mass centers after auto and manual plant tracing were calculated [Table 2].

The study has shown that the mean distances between the circle center and mass center of the plants were 18 pixels and 21 pixels, respectively. These values indicate a high degree of accuracy in identifying the plants.

However, it should be noted that the quality of the images used in the study posed a challenge for manual tracing. This was due to the unclear edges of the lettuce plants in most cases. As a result, the ground truth data obtained cannot be considered 100% accurate.

#	Circle and Mass centers after manual tracing				Circle and Mass centers after auto plant identification					
	Circle center X1 (pixels)	Circle center Y1 (pixels)	Mass center X1 (pixels)	Mass center Y1 (pixels)	Circle center X2 (pixels)	Circle center Y2 (pixels)	Mass center X2 (pixels)	Mass center Y2 (pixels)	Circle center distance (pixels)	Mass center distance (pixels)
1	426	451	423	454	437	448	448	460	12	26
2	455	504	450	508	443	509	438	517	14	16
3	420	461	417	461	430	480	424	497	21	37
4	435	494	435	496	435	476	432	492	19	5
5	412	490	414	491	432	499	436	507	21	28
6	412	526	415	538	422	530	434	549	10	22
7	439	491	437	493	440	490	444	511	1	19
8	468	484	471	482	449	488	442	504	19	36
9	428	545	430	550	426	542	421	556	4	11
10	436	496	440	496	431	468	430	486	28	14
11	420	497	415	498	439	507	447	522	22	40
12	407	474	413	476	423	459	429	462	22	22
13	423	466	418	466	441	505	444	537	42	75
14	443	482	441	491	449	466	452	493	17	11
15	448	505	452	509	438	462	435	482	44	32
16	416	493	420	496	408	454	409	471	40	28
17	441	483	447	494	448	499	457	518	17	27
18	425	470	419	470	435	477	426	498	12	29
19	442	558	445	560	460	523	457	528	39	35
20	435	535	439	540	437	508	440	535	27	5
21	405	493	412	495	421	487	428	493	17	17
22	420	510	414	510	426	499	416	516	12	7
23	403	506	406	513	426	496	431	511	25	25
24	391	554	389	560	397	517	399	542	38	20
25	441	497	446	501	435	483	436	509	16	13
26	410	445	406	445	430	454	428	475	21	37
27	409	438	414	441	422	431	424	437	16	10
28	403	491	400	494	406	480	398	513	11	19
29	431	507	435	512	423	488	423	517	21	13
30	417	446	413	446	442	458	443	478	28	43
31	405	465	411	466	419	462	422	470	14	11
32	391	505	389	508	391	506	382	538	0	31
33	423	509	430	518	442	491	446	503	26	22
34	473	474	477	477	461	475	466	497	12	22
35	411	444	419	446	423	441	437	449	12	18
36	463	419	466	416	457	422	456	434	8	20
37	456	429	456	433	475	425	470	444	20	18
38	424	461	431	471	430	472	426	490	12	20
39	433	508	435	505	437	511	434	510	5	5
40	440	500	440	500	430	498	433	500	11	7
41	442	499	443	498	443	500	445	497	2	1
42	430	551	430	551	443	563	444	562	17	18
43	440	561	440	561	444	562	445	564	3	6
								Mean Distance	18	21

Table 2.

Distance between circle and mass centers after auto and manual plant tracing

6. Application of the system

6.1. Experimentation with plant growth monitoring

An experiment was performed, monitoring and recording lettuces as they grew over the weeks.

The monitoring of young lettuces started at 12/5/22, and continued at 19/5/22, at 28/5/22 and finally at 3/6/22.

The system, proved to be quite capable of recognizing the plants, isolating and centering them in the camera's field of view.

Images [Image 77 through Image 92], show four lettuces as they grew over the weeks.

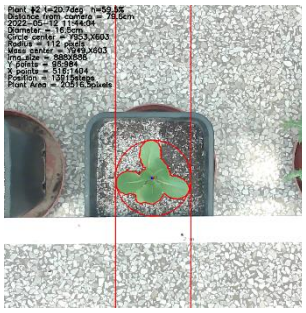

Image 77.
12/5/22 1st lettuce

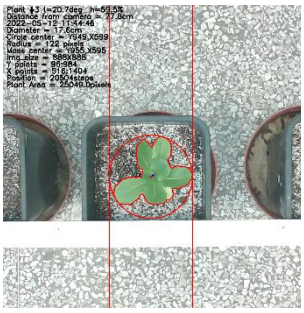

Image 78.
12/5/22 2nd lettuce

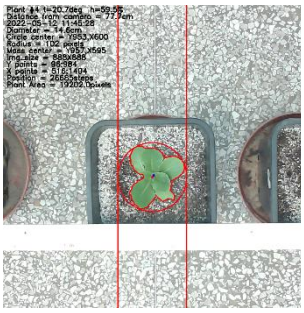

Image 79.
12/5/22 3rd lettuce

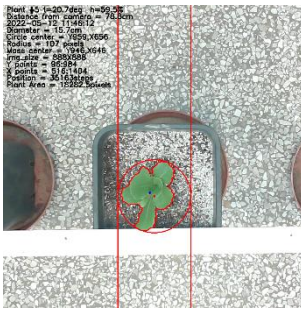

Image 80.
12/5/22 4th lettuce

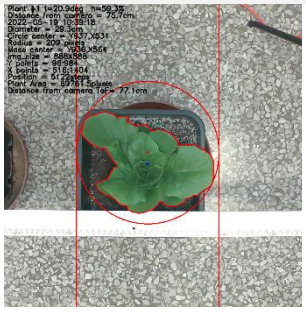

Image 81.
19/5/22 1st lettuce

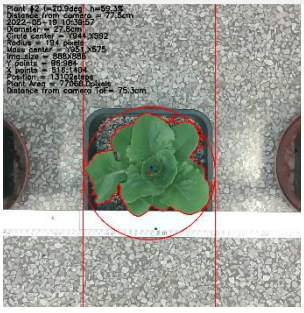

Image 82.
19/5/22 2nd lettuce

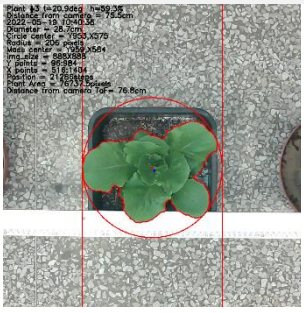

Image 83.
19/5/22 3rd lettuce

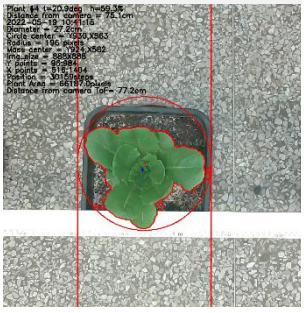

Image 84.
19/5/22 4th lettuce

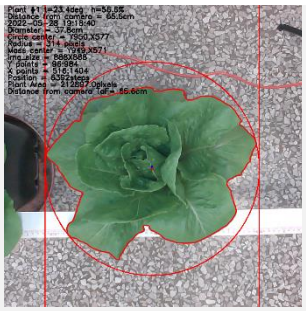

Image 85.
28/5/22 1st lettuce

Image 86.
28/5/22 2nd lettuce

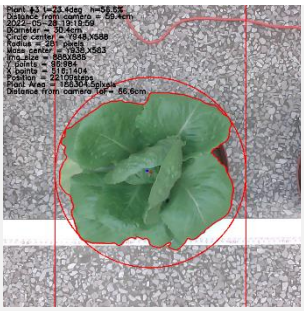

Image 87.
28/5/22 3rd lettuce

Image 88.
28/5/22 4th lettuce

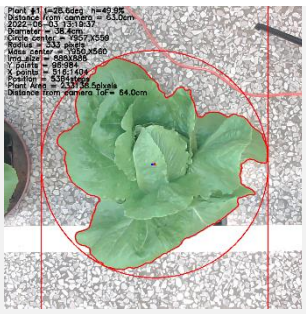

Image 89.
3/6/22 1st lettuce

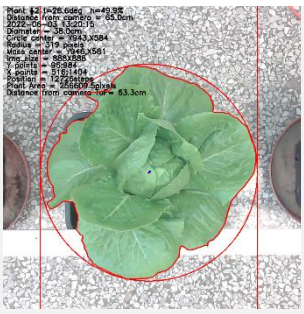

Image 90.
3/6/22 2nd lettuce

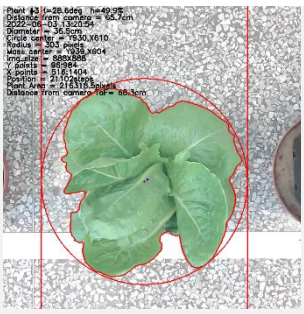

Image 91.
3/6/22 3rd lettuce

Image 92.
3/6/22 4th lettuce

Due to limitations in the lab's ability to provide adequate sunshine, the lettuces were transferred between the lab and greenhouse environments back and forth, and each time the system was set to perform a single Photo Sequence, keeping about the same lighting conditions in the lab and without changing the parameters of RoboPlantDect.

Not having to manually set the plant positions to the system, or to place each lettuce in the exact same spot as the previous Photo Sequence, proved to be very convenient!

The actions that had to be undertaken were:

- place the lettuces directly under the aluminum beam, in a manner that they were not overlapping each other
- using the user interface, select the number of plants
- make sure that the "Autofind" checkbox is checked
- press the "Photo Sequence" button

All of the parameters needed were carefully selected only the first time.

6.2. MEF producing HDR images

6.2.1. Introduction to HDR

In a greenhouse environment, the lighting conditions can fluctuate significantly over the course of a day, which can present challenges for systems designed to detect and monitor plant growth. These variations are influenced by a range of factors, including weather conditions such as cloud cover, as well as the angle of the sunrays as they penetrate the greenhouse structure.

To ensure that accurate plant detection can be achieved despite these lighting variations, it is necessary to make adjustments to the color and exposure thresholds of the system, every time the lighting conditions are altered, raising a serious issue.

One approach to addressing this issue is to operate the system exclusively at night, when the only available light source is the system's own LEDs. By doing so, the lighting conditions can be kept consistent, and the thresholds can be set initially and then remain unchanged in the future.

Another approach to addressing this issue is to use Multi-exposure image fusion (MEF) to produce a High Dynamic Range Imaging (HDR) image, a method that involves acquiring multiple images of the same scene with different lighting conditions or exposure times and then combining them into a single image that simulates perfect lighting conditions. This method can help to address the challenges posed by lighting variations and produce more accurate images of plant growth.

However, producing an HDR image is not enough in itself, as the image will need to undergo Tone Mapping to produce a more realistic image. Tone mapping is a technique used in image processing and computer graphics to display a high dynamic range (HDR) image on a low dynamic range (LDR) display.

HDR images contain a wider range of brightness values than can be displayed on a standard monitor or print. Tone mapping algorithms are used to compress the range of values in the HDR image into the limited range of the LDR display while preserving the important visual details and overall appearance of the original image.

OpenCV (OpenCV HDR, n.d.) provides several Tone Mapping algorithms, including Drago Tonemap, Simple Tonemap, Reinhard Tonemap, and Mantiuk Tonemap, all of which are explored and tested to find the most effective solution.

To test the effectiveness of different exposure times and lighting conditions, two experiments were conducted.

6.2.2. MEF with normal lighting conditions

With lighting conditions of a well illuminated office, ten images were acquired with different exposure times, specifically:
1ms, 3ms, 5ms, 10ms, 50ms, 0.1s, 0.5s, 1s, 3s, 5s respectively, [Image 93. through Image 102.].

Image 93.
1ms exposure

Image 94.
3ms exposure

Image 95.
5ms exposure

Image 96.
10ms exposure

Image 97.
50ms exposure

Image 98.
0.1s exposure

Image 99.
0.5s exposure

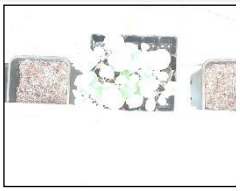

Image 100.
1s exposure

Image 101.
3s exposure

Image 102.
5s exposure

Obviously, as it can be seen at images [Image 97, Image 98], 50ms and 0.1s exposure times produce the best images for these specific lighting conditions. The lower exposure times produce underlit images, and the higher exposure times produce overlit images.

It is self-explanatory that:

- When lighting is very low, e.g. no other lighting source other than the system's LEDs, higher exposure times will produce the best images, while lower exposure times will produce excessively underlit images.
- When lighting is extreme, e.g. direct sunlight, higher exposure times will produce excessively overlit images, while lower exposure times will produce better images.

Using OpenCV's functions, combining all these images, an HDR image is produced [Image 103]. While an HDR image contains all the necessary information about the scene, it may not appear visually pleasing due to its unrealistic colors. Tone mapping is the process of compressing the dynamic range of an HDR image to fit within the limited range of brightness that can be displayed on a monitor or printed. Tone mapping algorithms are designed to produce an image with pleasing visual appearance while maintaining the contrast and detail of the original HDR image.

Image 103.
HDR image produced

OpenCV provides several tone mapping algorithms that can be used to enhance the appearance of HDR images.
The tone mapping algorithms that have been applied, are Drago Tonemap [Image 104], Mantiuk Tonemap [Image 105], Reinhard Tonemap [Image 106] and Simple Tonemap [Image 107].

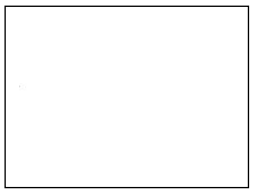

Image 104.
Drago Tonemap

Image 105.
Mantiuk Tonemap

Image 106.
Reinhard Tonemap

Image 107.
Simple Tonemap

Clearly, Drago Tonemap [Image 104], produced a blank image, and Mantiuk Tonemap [Image 105], produced a rather bad image, both of which are not acceptable.

Reinhard Tonemap [Image 106] produced the most promising results among the tested algorithms. However, it was observed that the colors in the output appeared to be slightly smeared.

6.2.3. MEF with very poor lighting conditions

Another experiment has been performed, at the same location, this time with very poor lighting conditions. Essentially, the only lighting source provided was the system's LEDs.

Nine images were acquired, but this time with different exposure times, specifically: 10ms, 50ms, 0.1s, 0.5s, 0.625s, 1s, 1.25s, 3s, 5s respectively, [Image 108 through Image 116].

Image 108.
10ms exposure

Image 109.
50ms exposure

Image 110.
0.1ms exposure

Image 111.
0.5s exposure

Image 112.
0.625s exposure

Image 113.
1s exposure

Image 114.
1.25s exposure

Image 115.
3s exposure

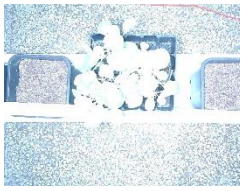

Image 116.
5s exposure

From these images, the HDR image produced can be shown in [Image 117].

Image 117.
HDR image produced

Once again, the tone mapping algorithms that have been applied: Drago Tonemap [Image 118], Mantiuk Tonemap [Image 119], Reinhard Tonemap [Image 120] and Simple Tonemap [Image 121].

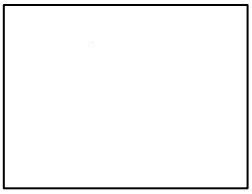

Image 118.
Drago Tonemap

Image 119.
Mantiuk Tonemap

Image 120.
Reinhard Tonemap

Image 121.
Simple Tonemap

As with the previous experiment, Drago Tonemap [Image 104], produced a blank image and Mantiuk Tonemap [Image 105], produced a rather bad image, both of which are not acceptable.

Like the previous experiment, Reinhard Tonemap [Image 106] produced the best results, and this time the colors appear to be more accurate.

6.2.4. Conclusions about Multi-exposure image fusion (MEF)

Multi-exposure image fusion (MEF) Imaging is a powerful technique that has the potential to provide consistent image quality, regardless of the lighting conditions in the greenhouse.

With the ability to capture a wide range of brightness values, HDR images produced with MEF can capture details that would otherwise be lost in high contrast situations, making it an ideal choice for greenhouse imaging. However, while this method has many benefits, it is not without its challenges.

One of the primary challenges associated with Multi-exposure image fusion is the time it takes to acquire an image. The process of capturing multiple exposures and combining them into a single HDR image can be time-consuming, taking more than ten seconds for every time an image is to be acquired, either for detecting the plant, or for taking the final picture of it.

Another challenge is the color quality of the produced images. HDR images can result in color shifts due to the processing algorithms used. As such, further experimentation and tweaking are to be explored.

Ultimately, this method has not been implemented to the system, but should the researchers require, such an implementation can easily be done later on in the future.

6.3. Calculation of NDVI index

6.3.1. Introduction to NDVI

Normalized Difference Vegetation Index (GSIS Geography NDVI, n.d.) is a widely used formula in remote sensing and precision agriculture for determining the health and growth status of vegetation. NDVI is calculated using near-infrared (NIR) and red light, and is expressed as the ratio of the difference between NIR and red light to their sum. The formula for NDVI is as follows:

$$NDVI = \frac{NIR - Red}{NIR + Red}$$

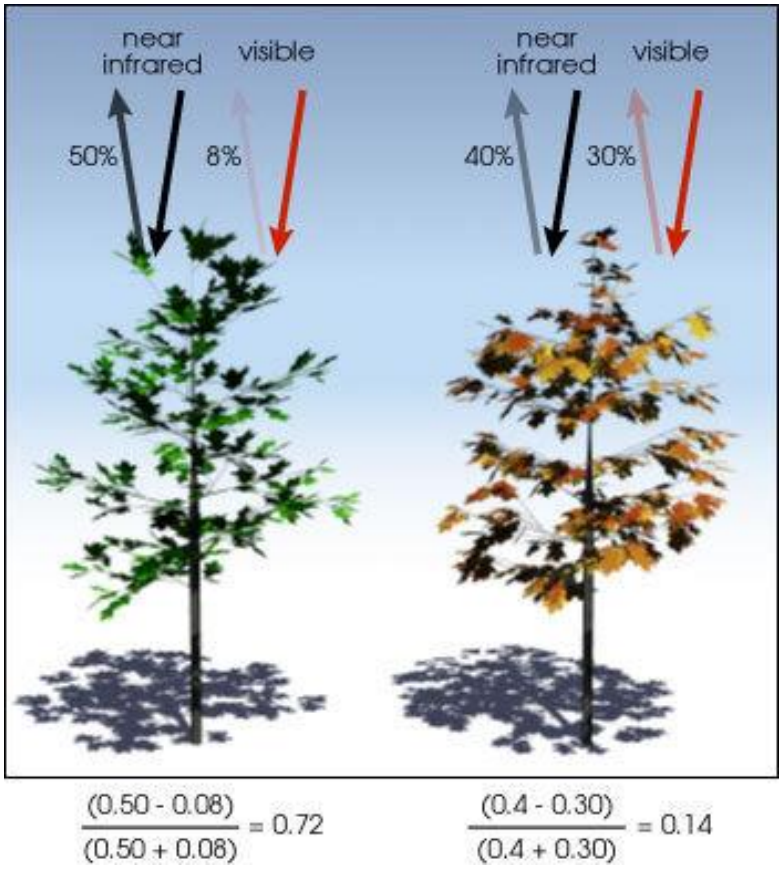

Image 122.
Normalized Difference Vegetation Index (NDVI), (source: gisgeography.com)

NDVI values range between -1 and +1, with higher values indicating healthy vegetation and lower values indicating stressed or unhealthy vegetation. NIR values are obtained

from specialized NIR images, while red values are derived from the red channel of RGB images, for each pixel of the image.

Healthy vegetation strongly reflects NIR light and absorbs red light [Image 122], resulting in high NDVI values. Conversely, water and other non-vegetated surfaces typically have lower NDVI values. The high sensitivity of NDVI to vegetation health has made it a valuable tool for monitoring plant growth and detecting stress in individual plants and larger areas.

NDVI is commonly used with satellite images to monitor vegetation health and growth over large areas. However, it is also used in precision agriculture for individual plants, as the human eye is not able to detect the subtle differences in plant health that NDVI can capture. The reflected infrared light from plants decreases as their health deteriorates, making NDVI images a valuable tool for identifying and addressing plant stressors such as nutrient deficiencies, watering imbalances, and insufficient sunlight exposure [Figure 15].

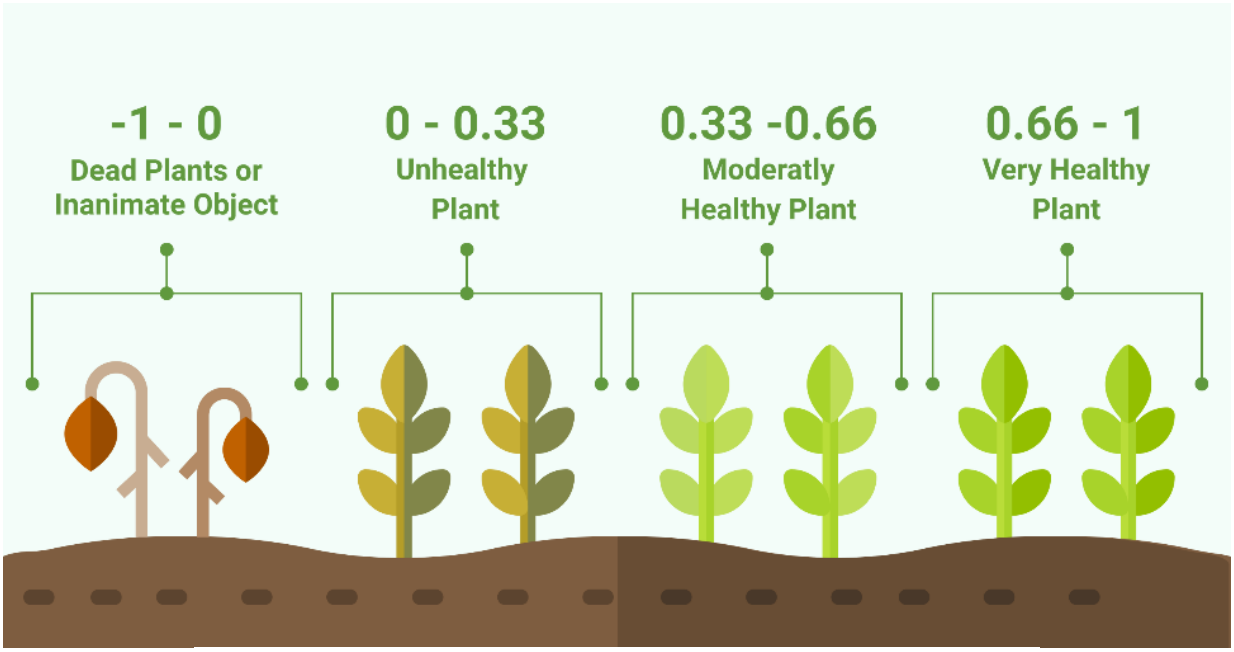

Figure 15.
NDVI Plant Classification (source: phenospex.com)

In conclusion, NDVI is a powerful tool for assessing the health and growth status of vegetation, with applications ranging from large-scale monitoring of crop health to individual plant analysis in precision agriculture. The ability to measure subtle differences in reflectance and health status has made NDVI an indispensable tool for plant monitoring and management.

6.3.2. Image alignment for acquiring NDVI

There has been an experimentation for acquiring NDVI images.

Image 123.
RGB image for acquiring NDVI

Image 124.
NIR image for acquiring NDVI

Images from both RGB [Image 123] and NIR [Image 124] cameras were acquired.

There is a distance between the RGB and the NIR camera, specifically, 14.82mm, so the carriage has been moved in an attempt to align the two images. However, this was not enough, since the two cameras, are not identical. The two lenses produce a slightly different image, so in order to achieve the best results possible, Homography (learnopencv Image Alignment in OpenCV, n.d.) image alignment was applied before applying the NDVI formula.

By applying the NDVI formula to the above images, a black and white image resulted [Image 125].

A color filter was applied to this image so that the user can easily distinguish the differences of the reflected light, thus, the health of the plant [Image 126].

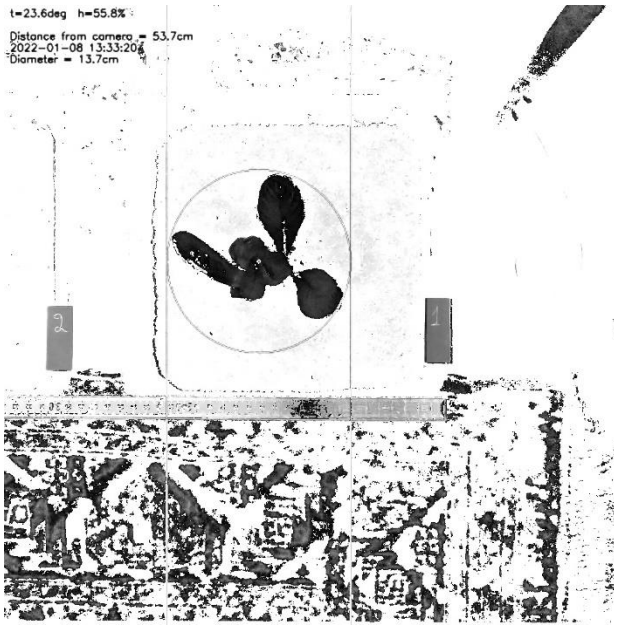

Image 125.
NDVI result

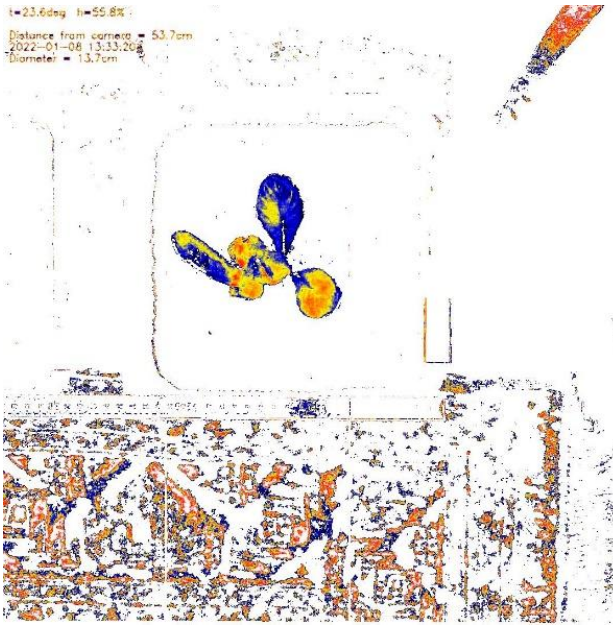

Image 126.
NDVI result after applying a color filter

The two different cameras raise difficulties for acquiring NDVI images.

All the problems would have been eliminated if there was a single camera capable of acquiring both NIR and RGB images simultaneously. One lens as well as one sensor, will produce perfectly aligned images, without the need of Homography, or other alignment techniques.

7. Discussion and conclusions

The system demonstrated excellent performance for long-term monitoring of plants.

- When configured properly and used under consistent lighting conditions, the system can provide valuable support for researchers and agronomists. Specifically, it can automatically detect and identify plants, acquire centered images of them, and perform basic measurements.
- The repeatability of the procedures conducted using the system is excellent, and its user-friendly options facilitate proper configuration.
- Despite its high functionality, the system is light enough to be easily lifted, moved, and set up in a greenhouse by a single person.
- Remote operation is possible, enabling users to control the system from anywhere in the world.
- The system is modular, with aluminum beams adding up to a length of 3.5m. By adding or subtracting beams, the system can be easily adjusted to lengths ranging from 1m up to 5m.
- The system requires only a 230V AC and a Wi-Fi source to operate, making it highly convenient for users.

However, there is still room for improvement in several areas:

- The user interface, while functional, can be slow and requires careful attention to avoid accidentally clicking the wrong button. Exploring different UI libraries may help address this issue.
- Distance sensors used to measure plant diameter and area were found to be occasionally inaccurate. Upgrading to more precise, albeit expensive, laser distance sensors may offer a solution.
- A more powerful stepper motor would improve the carriage's speed, enhancing overall system performance.
- Upgrading to a more powerful computing system such as the NVIDIA® Jetson Nano™ would substantially reduce the computing time required for image processing.
- Using more powerful LEDs would improve lighting conditions for image capturing, resulting in higher-quality images and more accurate plant identification.
- Utilizing a camera that has RGB and IR pixels in the same sensor, the system would be able to provide the researchers with a perfect NDVI image, which will be quite useful, showing the plants' health in a manner that can't be compared to the observation of a plain RGB image.

8. Future work

RoboPlantDect is a basic system that opens a lot of possibilities:

- If a camera capable of acquiring IR and RGB images using the same lens and sensor, then the NDVI calculated will be perfect, thus implementing such a calculation in the system.

- Multi-exposure image fusion (MEF) producing High Dynamic Range Imaging (HDR) images, can be a "life saver" regarding the lighting conditions, so, after tweaking and improvements, it can be embedded in RoboPlantDect.

- A depth camera could be included to explore the accuracy of the distance measurement.

- Machine learning could be implemented, thus eliminating the need for manual thresholding of HSV.

- Humidity sensors and watering valves connected to a wireless microcontroller could be implemented to the system, in order to make the plant growing a truly automated process.

- By adding an elliptical beam perpendicular to the existing one, the camera could get images of the plant from various angles, thus providing the ability of the 3d reconstruction of the plant.

References

AnyDesk. (n.d.). Retrieved from https://anydesk.com/en

Big Data in Smart Farming – A review. (n.d.). p. https://doi.org/10.1016/j.agsy.2017.01.023.

Chlorophyll estimation in soybean leaves infield with smartphone digital imaging and machine learning. (n.d.). p. https://doi.org/10.1016/j.compag.2020.105433.

CNN World: Is the biggest greenhouse in the US the future of farming? (n.d.). Retrieved from https://edition.cnn.com/2021/10/06/world/appharvest-kentucky-greenhouse-robot-farming-spc-intl-hnk/index.html

cvui 2.7.0. (n.d.). Retrieved from https://dovyski.github.io/cvui/

EasyEDA. (n.d.). Retrieved from https://easyeda.com/

GSIS Geography NDVI. (n.d.). Retrieved from https://gisgeography.com/ndvi-normalized-difference-vegetation-index/

Hue Saturation Value (HSV) Color Space. (n.d.). Retrieved from https://www.youtube.com/watch?v=4Kvefi8_wls

ImageJ. (n.d.). Retrieved from https://github.com/imagej

learnopencv Image Alignment in OpenCV. (n.d.). Retrieved from https://learnopencv.com/image-alignment-ecc-in-opencv-c-python/

Machine learning approaches for crop yield prediction and nitrogen status estimation in precision agriculture: A review. (n.d.). p. http://dx.doi.org/10.1016/j.compag.2018.05.012.

NDVI. (n.d.). pp. https://gisgeography.com/ndvi-normalized-difference-vegetation-index/.

NDVI. (n.d.). Retrieved from https://gisgeography.com/ndvi-normalized-difference-vegetation-index/

OpenCV. (n.d.). Retrieved from https://opencv.org

OpenCV HDR. (n.d.). Retrieved from https://docs.opencv.org/4.x/d3/db7/tutorial_hdr_imaging.html

OpenDV Camera Calibration. (n.d.). Retrieved from https://learnopencv.com/camera-calibration-using-opencv/

scantips Calculate Distance or Size of an Object in a photo image. (n.d.). Retrieved from https://www.scantips.com/lights/subjectdistance.html

Syncthing. (n.d.). Retrieved from http://www.syncthing.net

VNC® Server. (n.d.). Retrieved from https://www.realvnc.com/en/connect/download/vnc/

VNC® Viewer. (n.d.). Retrieved from https://www.realvnc.com/en/connect/download/viewer/

Wikipedia: Greenhouse. (n.d.). Retrieved from https://en.wikipedia.org/wiki/Greenhouse

Wikipedia: History of agriculture . (n.d.). Retrieved from https://en.wikipedia.org/wiki/History_of_agriculture

Zhang, L., Xu, Z., Xu, D., Ma, J., Chen, Y., & Fu, Z. (2020). Growth monitoring of greenhouse lettuce based on a convolutional neural network. Horticulture Research, 7(1), 1-12. https://doi.org/10.1038/s41438-020-00345-6

Li, H., Guo, Y., Zhao, H., Wang, Y., & Chow, D. (2021). Towards automated greenhouse: A state of the art review on greenhouse monitoring methods and technologies based on internet of things. Computers and Electronics in Agriculture, 191, 106558. https://doi.org/10.1016/j.compag.2021.106558

Bauer, A., Bostrom, A. G., Ball, J., Applegate, C., Cheng, T., Laycock, S., Rojas, S. M., Kirwan, J., & Zhou, J. (2019). Combining computer vision and deep learning to enable ultra-scale aerial phenotyping and precision agriculture: A case study of lettuce production. Horticulture Research, 6(1), 1-10. https://doi.org/10.1038/s41438-019-0151-5

Moschou, C. E., Papadimitriou, D. M., Galliou, F., Markakis, N., Papastefanakis, N., Daskalakis, G., Sabathianakis, M., Stathopoulou, E., Bouki, C., Daliakopoulos, I. N., & Manios, T. (2022). Grocery waste compost as an alternative hydroponic growing medium. Agronomy, 12(4), 789. https://doi.org/10.3390/agronomy12040789

Nikoloudakis, Y., Panagiotakis, S., Manios, T., Markakis, E., & Pallis, E. (2018). Composting as a Service: A Real-World IoT Implementation. Future Internet, 10(11), 107. https://doi.org/10.3390/fi10110107

Nikoloudakis, Y., Panagiotakis, S., Markakis, E., Atsali, G., & Manios, T. (2016). Cloud Composting: A Centralised Approach. In 2016 7th International Conference on Telecommunications and Multimedia (TEMU) (pp. 1-5). IEEE. https://doi.org/10.1109/TEMU.2016.7551941

Fragkopoulos, M., Panagiotakis, S., Kostakis, M., Markakis, E. K., Astyrakakis, N., & Malamos, A. (2023). Experimental assessment of common crucial factors that affect LoRaWAN performance on suburban and rural area deployments. Sensors, 23(3), 1316. https://doi.org/10.3390/s23031316

Kamarianakis, Z., & Panagiotakis, S. (2023). Design and Implementation of a Low-Cost Chlorophyll Content Meter. Sensors, 23(5), 2699. https://doi.org/10.3390/s23052699

Ahsan, M., Eshkabilov, S., Cemek, B., Küçüktopcu, E., Lee, C. W., & Simsek, H. (2022). Deep Learning Models to Determine Nutrient Concentration in Hydroponically Grown Lettuce Cultivars (Lactuca sativa L.). Sustainability, 14(1), 416. https://doi.org/10.3390/su14010416

Moraitis, M., Vaiopoulos, K., & Balafoutis, A. T. (2022). Design and Implementation of an Urban Farming Robot. Micromachines, 13(2), 250. https://doi.org/10.3390/mi13020250

Zeidler, C., Zabel, P., Vrakking, V., Dorn, M., Bamsey, M., Schubert, D., Ceriello, A., Fortezza, R., Simone, D., Stanghellini, C., Kempkes, F., Meinen, E., Mencarelli, A., Swinkels, G. J., Paul, A. L., & Ferl, R. J. (2019). The Plant Health Monitoring System of the EDEN ISS Space Greenhouse in Antarctica During the 2018 Experiment Phase. Frontiers in Plant Science, 10, 1457. https://doi.org/10.3389/fpls.2019.01457

Birrell, S., Hughes, J., Cai, J. Y., & Iida, F. (2019). A field-tested robotic harvesting system for iceberg lettuce. Journal of Field Robotics, 37(2), 225-245. https://doi.org/10.1002/rob.21888

Rajalakshmi, T. S., Panikulam, P., Sharad, P. K., & Nair, R. R. (2021). Development of a small scale cartesian coordinate farming robot with deep learning based weed detection. Journal of Physics: Conference Series, 1969, 012007.

Zhang, Z. Y. (2000). A flexible new technique for camera calibration. IEEE Transactions on Pattern Analysis and Machine Intelligence, 22(11), 1330-1334.

Heikkila, J., & Silvén, O. (1997). A four-step camera calibration procedure with implicit image correction. In Proceedings of the IEEE Computer Society Conference on Computer Vision and Pattern Recognition (pp. 1106-1112).

cvui. (n.d.). Computer Vision User Interface. Retrieved January 10, 2022, from https://dovyski.github.io/cvui/

Story, D., & Kacira, M. (2015). Design and implementation of a computer vision-guided greenhouse crop diagnostics system. Machine Vision and Applications, 26, 495-506.

Story, D., & Kacira, M. (2013, October). Automated machine vision guided plant monitoring system for greenhouse crop diagnostics. In International Symposium on New Technologies for Environment Control, Energy-Saving and Crop Production in Greenhouse and Plant 1037 (pp. 635-641).

Jayasekara, C., Banneka, S., Pasindu, G., Udawaththa, Y., Wellalage, S., & Abeygunawardhane, P. K. (2021, December). Automated Crop Harvesting, Growth Monitoring and Disease Detection System for Vertical Farming Greenhouse. In 2021 3rd International Conference on Advancements in Computing (ICAC) (pp. 228-233). IEEE.

Tang, Y., Chen, M., Wang, C., Luo, L., Li, J., Lian, G., & Zou, X. (2020). Recognition and localization methods for vision-based fruit picking robots: A review. Frontiers in Plant Science, 11, 510. https://doi.org/10.3389/fpls.2020.00510

Ehret, D., Lau, A., Bittman, S., Lin, W., & Shelford, T. (2001). Automated monitoring of greenhouse crops. Agronomie, 21(4), 403-414. https://doi.org/10.1051/agro:2001133

McCarthy, C. L., Hancock, N. H., & Raine, S. R. (2010). Applied machine vision of plants: a review with implications for field deployment in automated farming operations. Intelligent Service Robotics, 3, 209-217. https://doi.org/10.1007/s11370-010-0070-9

Sudkaew, N., & Tantrairatn, S. (2021, November). Foliar Fertilizer Robot for Raised Bed Greenhouse Using NDVI Image Processing System. In 2021 25th International Computer Science and Engineering Conference (ICSEC) (pp. 222-227). IEEE. https://doi.org/10.1109/ICSEC51691.2021.9527975

Reyes-Yanes, A., Martinez, P., & Ahmad, R. (2020). Real-time growth rate and fresh weight estimation for little gem romaine lettuce in aquaponic grow beds. Computers and Electronics in Agriculture, 179, 105827. https://doi.org/10.1016/j.compag.2020.105827

Belforte, G., Deboli, R., Gay, P., Piccarolo, P., & Aimonino, D. R. (2006). Robot design and testing for greenhouse applications. Biosystems Engineering, 95(3), 309-321. https://doi.org/10.1016/j.biosystemseng.2006.06.003

Bahman, L. (2019). Height measurement of basil crops for smart irrigation applications in greenhouses using commercial sensors (Doctoral dissertation, The University of Western Ontario (Canada)). https://ir.lib.uwo.ca/etd/6162/

Lu, Y., & Young, S. (2020). A survey of public datasets for computer vision tasks in precision agriculture. Computers and Electronics in Agriculture, 178, 105760. https://doi.org/10.1016/j.compag.2020.105760

Kushwaha, H. L. (2019). Robotic and mechatronic application in agriculture. RASSA Journal of Science for Society, 1(3), 89-97. https://doi.org/10.21567/rjss.v1i3.52570

Sollazzo, A., Colliaux, D., Garivani, S., Minchin, J., Garlanda, L., & Hanappe, P. (2020). Automated vegetable growth analysis from outdoor images acquired with a cablebot. In Proceedings of the IEEE International Conference on Computer Vision Workshops.

Kacira, M., & Ling, P. P. (2001). Design and development of an automated and non-contact sensing system for continuous monitoring of plant health and growth. Transactions of the ASAE, 44(4), 989-996.

Burns, J. I. (2014). Agricultural crop monitoring with computer vision (Doctoral dissertation). Virginia Tech.

Vázquez-Arellano, M., Reiser, D., Paraforos, D. S., Garrido-Izard, M., & Griepentrog, H. W. (2018). Leaf area estimation of reconstructed maize plants using a time-of-flight camera based on different scan directions. Robotics, 7(4), 63.

Wijanarko, A., Nugroho, A. P., Sutiarso, L., & Okayasu, T. (2019, December). Development of mobile RoboVision with stereo camera for automatic crop growth monitoring in plant factory. In AIP Conference Proceedings (Vol. 2202, No. 1, p. 020100). AIP Publishing LLC.

González-Esquiva, J. M., Oates, M. J., García-Mateos, G., Moros-Valle, B., Molina-Martínez, J. M., & Ruiz-Canales, A. (2017). Development of a visual monitoring system for water balance estimation of horticultural crops using low cost cameras. Computers and Electronics in Agriculture, 141, 15-26.

Van Henten, E. J., Bac, C. W., Hemming, J., & Edan, Y. (2013). Robotics in protected cultivation. IFAC Proceedings Volumes, 46(18), 170-177.

Luo, J., Li, B., & Leung, C. (2022). A Survey of Computer Vision Technologies In Urban and Controlled-Environment Agriculture. arXiv preprint arXiv:2210.11318.

Boatswain Jacques, A. (2019). Development of a machine vision-based yield monitoring system for vegetable crops.

Lu, X., Li, X., Chai, Y., & Li, X. (2014). Seedling image segmentation and feature extraction under complicated background. In Life System Modeling and Simulation: International Conference on Life System Modeling and Simulation, LSMS 2014, and International Conference on Intelligent Computing for Sustainable Energy and Environment, ICSEE 2014, Shanghai, China, September 20-23, 2014, Proceedings, Part I (pp. 387-399). Springer Berlin Heidelberg.

Kosmopoulos, D., Constantinopoulos, C., Papadimitriou, D., Manios, T., Fasoulas, J., Sfakiotakis, M., Stantoumis, C., Kalisperakis, I., Tsalavoutas, A., & Drikos, L. (2020). The soup project: Current state and future activities. International Journal of Interactive Systems and Smart Technologies, 11(1), 1-10. https://doi.org/10.26220/iisa.3343

Kounalakis, N., Kalykakis, E., Pettas, M., Makris, A., Kavoussanos, M. M., Sfakiotakis, M., & Fasoulas, J. (2021, June 11-13). Development of a Tomato Harvesting Robot: Peduncle Recognition and Approaching. In 2021 3rd International Congress on Human-Computer Interaction, Optimization and Robotic Applications (HORA) (pp. xx-xx). IEEE. https://doi.org/10.1109/HORA52670.2021.9461281

Georgantopoulos, P. S., Papadimitriou, D., Constantinopoulos, C., Manios, T., Daliakopoulos, I. N., & Kosmopoulos, D. (2023). A Multispectral Dataset for the Detection of Tuta Absoluta and Leveillula Taurica in Tomato Plants. Smart Agricultural Technology, 4, 100146. https://doi.org/10.1016/j.atech.2022.100146

Li, M. (2021). Research on color correction method of greenhouse tomato plant image based on high dynamic range imaging. INMATEH – Agricultural Engineering, 64(2), 393-402. https://doi.org/10.35633/inmateh-64-39